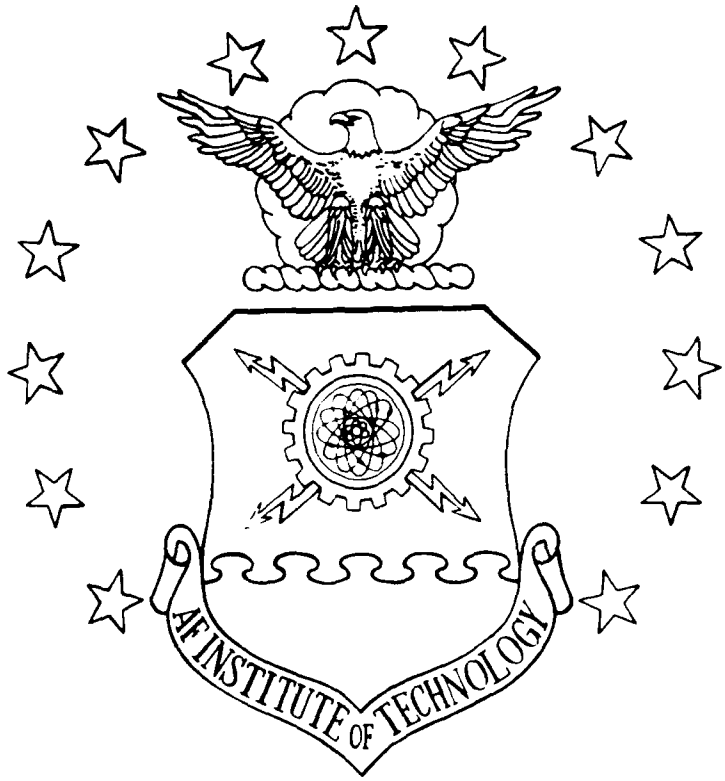

Use of Grasp Force Focus Positioning to Enhance the Torque Resistance Capability of Robotic Grasps

THESIS

Stephen G. Edwards
Capt USAF

AFIT/GA/ENY/90D-5

DEPARTMENT OF THE AIR FORCE
AIR UNIVERSITY
AIR FORCE INSTITUTE OF TECHNOLOGY

Wright-Patterson Air Force Base, Ohio

AFIT/GA/ENY/90D-5

Use of Grasp Force Focus Positioning to Enhance the Torque Resistance Capability of Robotic Grasps

THESIS

Stephen G. Edwards
Capt USAF

AFIT/GA/ENY/90D-5

Approved for public release; distribution unlimited

AFIT/GA/ENY/90D-5

Use of Grasp Force Focus Positioning to Enhance the Torque Resistance Capability of Robotic Grasps

THESIS

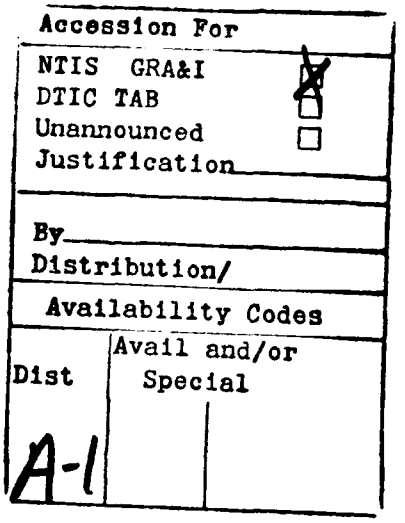

Presented to the Faculty of the School of Engineering

of the Air Force Institute of Technology

Air University

In Partial Fulfillment of the

Requirements for the Degree of

Master of Science in Astronautical Engineering

Stephen G. Edwards, B.S. in Astronautical Engineering

Capt USAF

December 13, 1990

Preface

This thesis could not have become a reality without the help and inspiration of several people. First and foremost there is Dr. Curtis Spenny, my advisor, whose idea it was to apply the grasp force focus positioning method (first presented by David Brock of MIT) to the torque resistance problem, and who was also always available for consultation, good-natured bantering, and a lofty idea or two. Capt. Paul Whalen was also of immeasurable help with various computer snags and software problems. . .I don't think I could have made it through the last two weeks without him. I'd also like to thank my committee members, Capt. Mike Leahy and Capt. Brett Ridgely, for their valuable inputs and assistance.

Finally, I'd like to thank Mom and Dad for their constant support, even though they were 4000 miles away, and also everyone I know named Jeff(3), John(2), Ken(2), and Bob(1) for those much-needed good times. If you're one of the above, and have a wife, be sure to tell her thanks for the occaisional home-cooked meal.

P.S. "It's *all* wrong!" *The Casual Observer*

Stephen G. Edwards

Table of Contents

List of Figures

Figure Page

List of Tables

Abstract

Three-point-contact grasps are unique in that the homogeneous solution for the contact forces always produces a grasp force focus. Careful positioning of this focus point in the grasp plane can help avoid two things; slipping at the contact points, and violation of joint torque limits. The focus placement method is explored theoretically be examining two types of grasps on cylinders; 1) fingertip grasps using three independently operated fingers, and 2) single-finger power grasps with one contact point on each of three links. Constraint maps are generated for various fingertip grasps in order to show how proper placement of the grasp force focus results in no-slip grasps. A specific single-finger power grasp (using a Utah/MIT Dextrous Hand (UMDH) finger) is examined in order to show that joint torque limits also affect focus placement. The results show that optimal focus location is grasp specific, and that torque direction also plays a role in the torque resistance capability of the grasp. The study is meant as a first step in enhancing the ability of dextrous hands to exert torques on cylindrical objects using power grasps.

Use of Grasp Force Focus Positioning to Enhance
the Torque Resistance Capability of Robotic Grasps

I. Introduction

1.1 Motivation

Many of the man-hour intensive tasks performed by U.S. military personnel in hostile environments could be accomplished more safely and efficiently with robots. In order to accomplish these tasks a robot must be capable of performing simple functions which humans often take for granted.

There exist, presently, dextrous manipulators which have the potential for performing simple maintenance tasks. However, these manipulators have limited capabilities because of the inability to "teach" them how to perform tasks that any human with basic motor skills could easily do. Describing how to perform such tasks to a machine, however, can be quite complicated.

One way of getting solutions to complex problems is to break the problem into parts, and find solutions to the parts one at a time. One of the most basic requirements for performing any task correctly is knowing how to grasp the object that is to be moved or manipulated. This problem can be further broken down into two categories; 1) what grasp geometry is required, and 2) how forces should be applied to the object and in what quantity. This project focuses on category 2, and the focus is further narrowed to tasks involving the application of torque to cylindrical objects.

This type of task was chosen because the results will contribute to the solution of a larger scale task currently being studied at AFIT; a task which demonstrates intelligent part mating skills. The specific task involves the use of robotic manipulators to affix an oil filter to a threaded post. This study is meant to focus on the last stage of the problem, which is torquing the filter so that it is seated tightly. The knowledge gained from this study can be built upon so that solutions of a more general nature may be found.

1.2 Objective

The grasp that a human uses to apply torque to a cylindrical object is called a power grasp [3:p1534]. The fingers are wrapped around the object in one direction, and the thumb in the other direction, and the palm is in contact with the object as well. This is a very complicated grasp to employ successfully with a robotic manipulator. In this study a simplifed grasp is employed using a three link finger wrapped around a small cylindrical object, with contacts on each of the three links. This grasp is described as a "single-finger power grasp". The goal is to use the method of grasp force focus positioning to find the contact force solution which gives the grasp the greatest ability to resist external torques or, equivalently, allows the manipulator to apply the most torque to the grasped object.

1.3 Problem Statement

Find the solution for the contact forces for a three-point power grasp of a cylindrical object that gives the manipulator the greatest ability to exert torque on the object. The solution must: maintain the equilibrium of the grasp, result in no slipping or loss of contact, and be within the capabilities of the manipulator.

1.4 Background

The idea of using grasp force placement as a method for improving manipulator capabilities was first presented in an article published in the IEEE Journal of Robotics and Automation in 1988 [2]. The author, David L. Brock, used grasp force focus positioning to initiate controlled slipping in robotic grasps, the goal being the enhancement of robot dexterity (object manipulation capabilities). The method was successfully applied to the Salisbury robot hand. The three-fingered hand was able to spin a cylindrical object about one of its transverse axes by simply altering the position of the grasp force forces in a controlled manner. In this case the external gravity force is used to induce the spin.

Application of Brock's method to the external torque resistance problem requires some modifications. This problem is essentially two-dimensional which allows some notation simplification and the elimination of torsional friction, etc. Also, there is a fundamental

difference in where the grasp force focus is placed. Brock places the focus in an area which produces the desired type of slipping. For this project, the goal is to place the focus in the stable area, and *avoid* slipping if at all possible.

In order to make the results more practical the limitations of the manipulator are taken into account. It is useless to command a manipulator to exert the contact forces needed to place the grasp force focus at a certain point if the manipulator is incapable of complying. Thus, the joint torques required to exert the contact forces must be calculated and compared to the maximum capabilities of the manipulator. This project examines a single-finger grasp with a contact point on each of the finger's three links. Therefore, a way is needed to calculate required joint torques when there are multiple contacts at different places on the finger.

Methods for calculating required joint torques for fingertip contacts are well documented [7:p656], [1:p77]. The problem becomes much more complex, however, when there are multiple contacts per finger. There is currently only a very limited amount of reference material dealing with multiple contact grasps [12], and none offer methods for calculating joint torques. However, this single-finger problem is fairly simple, and the joint torque calculation method for fingertip contacts can be modified and applied here.

1.5 Method of Approach

The solution for the contact forces can be broken into two parts; 1) the particular solution, and 2) the homogeneous solution. For this project the particular solution is constrained to be as small in magnitude as possible so that only one solution exists. The set of homogeneous contact forces, also known as the set of internal contact forces, has an infinitude of possible solutions. The goal is to see which homogeneous solution (in combination with the particular solution) results in the most torque resistance capability for the manipulator.

The method used to explore the possible homogeneous solutions involves the positioning of what is called the internal grasp force focus. The position of this focus will uniquely determine the homogeneous solution if the magnitude for the solution has been

set. In this way, a position of the focus in the grasp plane can be associated with a contact force solution. Conversely, the best contact force solution (when it is found) will have an associated position for the internal grasp force focus. This one-to-one correspondance is true, in the general case, only with three-point grasps.

The method used to determine which contact force solutions are best involves the application of test conditions to a representative subset of possible solutions. If the level of external torque on the object is low, then there will be a large number of solutions which pass the test conditions. This translates into a large area of the grasp plane where it is acceptable to place the grasp force focus. As the torque level is increased there become fewer and fewer acceptable solutions until only one remains. This solution can be determined graphically by finding the last acceptable grasp force focus location on the grasp plane.

Of course, the "best" solution will depend on the specific grasping problem which includes many different variables such as: 1) grasp geometry, 2) object size, 3) manipulator and object surface conditions, 4) the amount of external torque on the object, and 5) manipulator capabilities. First, fingertip grasps are used to explore how the first four variables effect the acceptable focus locations. Then, the single-finger power grasp is examined, taking into account the capabilities of the manipulator used for this project which consists of a single finger of the Utah/MIT Dextrous Hand (UMDH). The solution for the single-finger power grasp problem is a stepping stone toward finding the solution for the more complicated dextrous hand power grasp.

1.6 Contributions

The grasp force focus positioning method has great potential for the optimization of grasps that require stability. This project demonstrates the successful application of the method to a torque-resisting grasp, which is of immediate use to the AFIT Robotics Laboratory. However, there are many grasping problems where other types of forces and moments are involved, and grasp force focus positioning can be applied to these tasks as well. It is likely that this method will, in some form, be of use to the entire robotics community.

1.7 Organization

Chapter II will discuss the analysis behind the grasp force focus positioning method, and its application to the chosen grasp. A description of the computer program developed for this project is given in Chapter III, as well as some examples of output data. Chapter IV examines the results that were obtained for both the fingertip and single-finger grasps, and conclusions that can be drawn from these results are then discussed in Chapter V. Finally, Chapter VI gives recommendations for use of these results, and possible further study.

II. Grasp Analysis

2.1 The Grasp Matrix

A good place to start when analyzing a grasping problem is to look at the relationship between the *contact* forces and moments applied by the finger(s) to the grasped object, and the *external* forces and moments applied to the object by the environment. If the contact forces and moments (represented by $\bar{c}$) cause a static balance with the external forces and moments (represented by $\bar{F}$), then the two vectors can be related by the grasp matrix, W [6];

$$\bar{F} = W\bar{c} \tag{2.1}$$

where W depends on the configuration of the grasp.

2.2 Internal Grasping Forces

In general, for a non-square grasp matrix, given $\bar{F}$ and W it is possible to find a solution for $\bar{c}$ by using the pseudo-inverse of W (call it $W^{\#}$). If there is not a unique solution to $\bar{c}$ it is expected that the solution has particular and homogeneous parts.

$$\bar{c} = \bar{c}_p + \bar{c}_h \tag{2.2}$$

where;

$$\bar{c}_p = W^{\#}\bar{F} \tag{2.3}$$

The homogeneous portion of the solution represents the set of contact forces that exert no net force or moment on the grasped object. This means that $\bar{c}_h$ lies in the null space of W. If N is a matrix whose columns represent orthonormal basis vectors that span the null space of W, and λ is a vector of arbitrary magnitudes, then the solution to $\bar{c}_h$ can be represented as [5];

$$\bar{c}_h = N\lambda \tag{2.4}$$

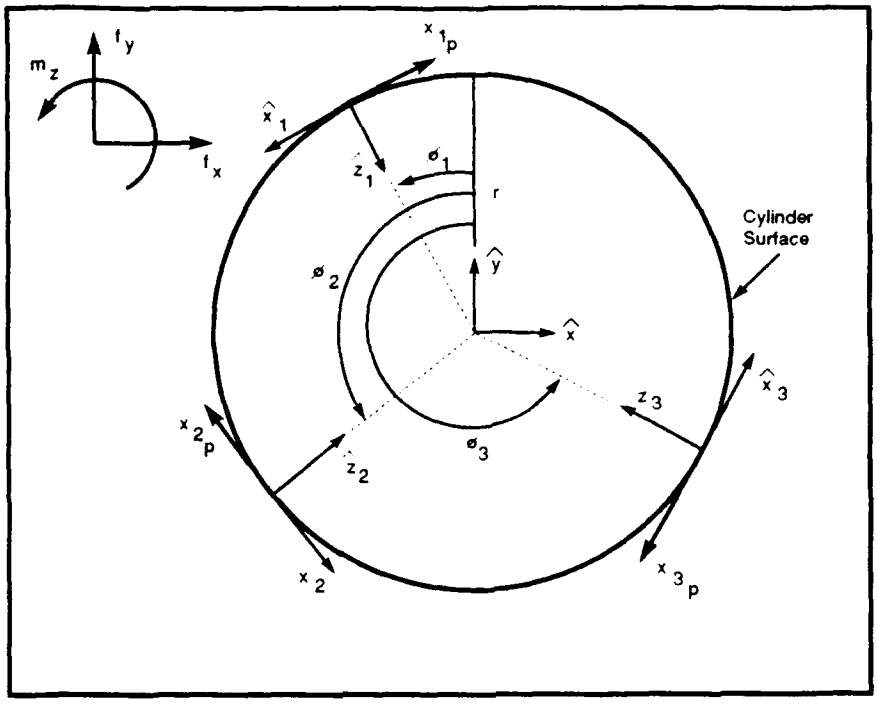

Figure 2.1. Balancing the External Moment

This vector, $\bar{c}_h$, represents what are called the internal grasping forces. In essence, $\bar{c}_p$ represents the forces needed to balance the environmental forces on the object, and the internal forces represent how much additional grasping force is exerted on top of that.

2.3 The Contact Force Particular Solution

For the special case which this project examines (i.e. a three-contact planar grasp of a cylindrical object) $\bar{c}_p$ need only be the tangential forces at the contact points required to balance the external moment about the object's longitudinal, or z-axis as shown in Figure 2.1. No normal components are required in this $\bar{c}_p$ solution. Analysis in [8] reveals that this solution for $\bar{c}_p$ produces a minimum norm set of components, as would be produced with the pseudo-inverse method. A valid particular solution for the contact forces is also constrained to balance external forces in the x- or y-directions. These three constraints; $\sum F_x = 0$, $\sum F_y = 0$, $\sum M_z = 0$, are applied to solve for the three tangential components of $\bar{c}_p$.

At this point component notation is introduced for the contact forces. Figure 2.1

shows a cylindrical object in a three-contact planar grasp. The "object" coordinate frame is located at the center of the cylinder with the z-axis pointing out of the page. This is not a true object frame since it does not rotate with the grasped cylinder, but stays in a fixed orientation with respect to the "world" frame. Orthogonal coordinate frames defined at each contact point with the z-axis normal to the cylinder, pointing inward, and the x-axis tangent to the cylinder in the counterclockwise direction. The positions of the contact points are defined by the angles ϕ_1, ϕ_2, ϕ_3, measured from the y-axis of the object frame, and by the radius of the object, r. The particular solution for the contact forces is represented by the three tangential force components x_{1_p}, x_{2_p}, and x_{3_p}, where the numerical subscripts denote the various contact points, and the "p" subscript indicates that this is the particular portion of the solution. The p subscript is necessary since it is possible to have tangential components as part of the homogeneous (internal) solution, and the two solution parts must be distinguished. As noted earlier, the normal components of the particular solution (z_{1_p}, z_{2_p}, and z_{3_p}) are zero.

Applying the three constraints to this system we obtain three equations in terms of the variables mentioned. In matrix form they are:

$$\begin{pmatrix} f_x \\ f_y \\ m_z \end{pmatrix} = \begin{bmatrix} cos\phi_1 & cos\phi_2 & cos\phi_3 \\ sin\phi_1 & sin\phi_2 & sin\phi_3 \\ -r & -r & -r \end{bmatrix} \begin{pmatrix} x_{1_p} \\ x_{2_p} \\ x_{3_p} \end{pmatrix} \tag{2.5}$$

Since this project focuses solely on how to counter a moment on the cylindrical object, we will assume that the environmental forces f_x, and f_y are zero. Having a square matrix in Equation 2.5 implies that the pseudoinverse is not needed to solve for the particular solution. Augmenting the matrix in Equation 2.5 and using Gaussian elimination readily yields the solution;

$$\begin{aligned} x_{1_p} &= \frac{B_1 B_2 - B_2 B_3}{B_1 B_4} \\ x_{2_p} &= \frac{B_1 B_5 - B_3 B_5}{B_5 B_4} \\ x_{3_p} &= \frac{B_5}{B_4} \end{aligned} \tag{2.6}$$

where;

$$
\begin{aligned}
B_1 &= cos\phi_2 - cos\phi_1 \\
B_2 &= cos\phi_2 - cos\phi_3 \\
B_3 &= cos\phi_3 - cos\phi_1 \\
B_4 &= sin(\phi_3 - \phi_2) + sin(\phi_2 - \phi_1) \\
&\quad + sin(\phi_1 - \phi_3) \\
B_5 &= -\frac{m_z}{r} cos\phi_2 \\
B_6 &= \frac{m_z}{r} cos\phi_1 \\
B_7 &= \frac{m_z}{r} sin(\phi_1 - \phi_2)
\end{aligned}
\tag{2.7}
$$

Therefore, given a moment, m_z, on a cylindrical object of radius r the contact forces needed to counter that moment can be found if the locations of the contact points are known.

As a check, common sense tells us that if the contact points are evenly spaced (what we will call a symmetrical grasp), then the values of x_{1_p}, x_{2_p}, and x_{3_p} should all be equal. Using Equations 2.6 and 2.7, and $\phi_1 = 0^o$, $\phi_2 = 120^o$, and $\phi_3 = 240^o$ we find that $x_{1_p} = x_{2_p} = x_{3_p} = \frac{-m_z}{3r}$, as expected.

2.4 The Internal Grasp Force Focus

As mentioned earlier, the internal grasp forces exert no net forces or moments on the grasped object. There is another unique characteristic of internal grasp forces, however, tnat is not as widely known. For a three-point grasp there are, in general, both normal and tangential components of the internal forces at each of the three contact points. If, at each contact point, these components are added, the net internal grasp force vector defines a line which lies in the plane of the grasp. If, at each of the three contact points, these lines are extended indefinitely in *both* directions it will always be true that these lines intersect at a single point [2]. This point is called the *internal grasp force focus*, also referred to herein as the "grasp force focus", or simply, "the focus".

The three contact points define the grasp plane, assuming the contact points are not

colinear, and the focus can lie anywhere on the grasp plane including points at infinity [2]. It is possible, using normalized internal force constraints, to prescribe where the grasp force focus will be in the grasp plane. However, the grasp force focus is defined only by the *directions* of the net internal forces at each contact point, and a unique homogeneous solution cannot exist until the magnitudes of those forces are specified.

2.5 The Internal Grasp Force Magnitude

Brock's definition for the internal grasp force magnitude, or simply, the grasp force magnitude was adopted for this project. Using my notation the definition is rewritten as;

$$m_g = \sqrt{x_{1_i}^2 + z_{1_i}^2} + \sqrt{x_{2_i}^2 + z_{2_i}^2} + \sqrt{x_{3_i}^2 + z_{3_i}^2} \tag{2.8}$$

where the "i" subscript denotes internal forces. Note that the contact force particular solution components do not contribute to m_g. Setting this magnitude at a desired value places another constraint on the internal forces, and there are now enough constraints to uniquely define a solution for the internal grasp force components.

2.6 The Homogeneous Solution

For a three point planar grasp there are six internal force components. This implies that six linearly independent constraints are needed to uniquely determine the homogeneous solution. The first three constraints are inherent in the definition of internal grasp forces; they must exert no net forces or moments on the grasped object. This implies that the sum of the forces in the x- and y-directions must equal zero, and the sum of the moments about the z-axis must equal zero. The fourth constraint comes from prescribing the value of the grasp force magnitude.

Three more constraints can be derived from the condition that at each contact point the net internal contact force must point directly toward (*or* directly away from) the prescribed grasp force focus. The position of the grasp force focus is given by grasp plane coordinates (x_g, y_g) where the x- and y-directions are as defined in Figure 2.2, and the origin is at the center of the cylinder.

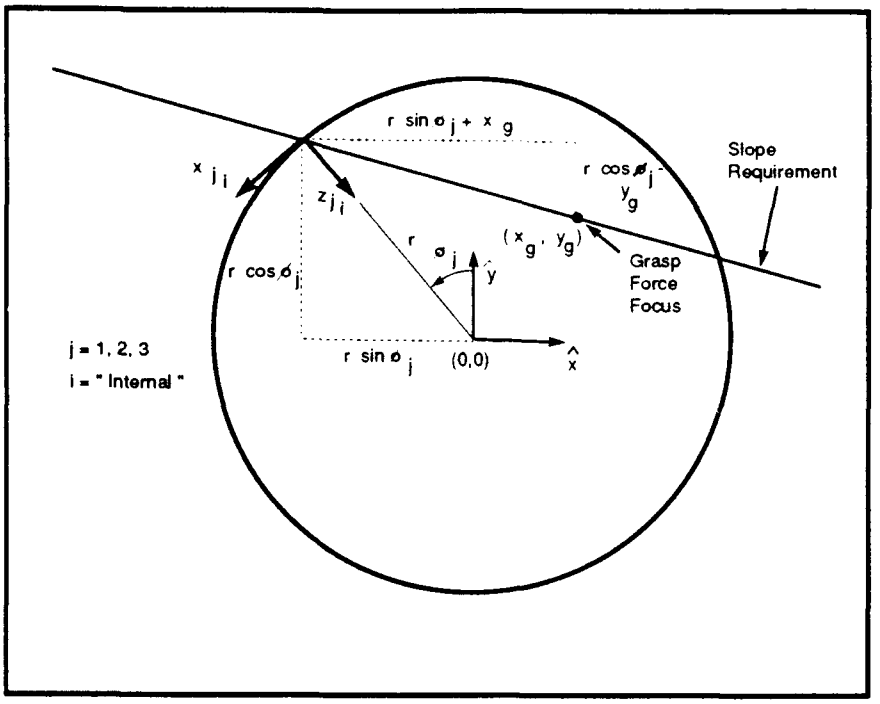

Figure 2.2. Prescribing the Grasp Force Focus Location

For the grasp force focus to be at (x_g, y_g), the horizontal (x) and vertical (y) internal force components at the jth contact point must obey the relationship

$$\frac{hoiz.\,comp.}{vert.\,comp.} = \frac{x_g + r\,sin\phi_j}{y_g - r\,cos\phi_j} \tag{2.9}$$

Translating the components to local contact frames, and simplifying, yields the three constraints;

$$(x_g sin\phi_j - y_g cos\phi_j + r)x_{j_i} + (x_g cos\phi_j + y_g sin\phi_j)z_{j_i} = 0 \qquad j = 1,2,3 \tag{2.10}$$

Now there are seven constraints, but Equation 2.8 does not lend itself to matrix form. Putting the six other constraints in matrix form reveals that they are linearly dependent, and any one of the constraints can be eliminated with elementary row operations. The five remaining equations in matrix form are used with Equation 2.8 as the six constraints needed to solve for the six internal contact force components. The five equations in matrix form are sufficient to solve for five of the components in terms of z_{j_i}. These five expressions

are substituted into Equation 2.8 which yields the solution for z_{3_i}. Equation 2.11 shows how back substitution is then used to get solutions for the other five components.

The process just outlined requires an extensive amount of algebra which is outlined in Appendix A. Parameterization allows the internal contact force solution to be shown with a reasonable amount of space. The P, Q, R, U, V, and W terms are the transitional parameters used.

$$\begin{aligned} z_{3_i} &= \frac{m_i}{\sqrt{W_1^2+W_2^2+1}\sqrt{W_3^2+W_4^2+1}\sqrt{W_5^2+1}} \\ x_{1_i} &= W_1 z_{3_i} \\ z_{1_i} &= W_2 z_{3_i} \\ x_{2_i} &= W_3 z_{3_i} \\ z_{2_i} &= W_4 z_{3_i} \\ x_{3_i} &= W_5 z_{3_i} \end{aligned} \tag{2.11}$$

where;

$$\begin{aligned} W_1 &= \frac{V_1}{P_5 Q_3 R_1} & W_4 &= \frac{V_4}{P_5 R_1} \\ W_2 &= \frac{V_2}{P_2 P_5 Q_3 R_1} & W_5 &= \frac{-P_7}{P_5} \\ W_3 &= \frac{V_3}{P_5 Q_3 R_1} \end{aligned} \tag{2.12}$$

where;

$$\begin{aligned} V_1 &= U_2 P_9 - U_1 P_{10} & V_3 &= U_6 P_9 - U_5 P_{10} \\ V_2 &= U_4 P_9 - U_3 P_{10} & V_4 &= R_6 P_9 - R_5 P_{10} \end{aligned} \tag{2.13}$$

where;

$$\begin{aligned} U_1 &= Q_3 R_1 - Q_5 R_1 + Q_5 R_5 & U_4 &= R_3 R_1 - R_1 R_6 \\ U_2 &= Q_1 R_6 - Q_6 R_1 & U_5 &= Q_5 R_1 - Q_1 R_5 \\ U_3 &= R_2 R_1 - R_1 R_5 & U_6 &= Q_6 R_1 - Q_1 R_6 \end{aligned} \tag{2.14}$$

where;

$$\begin{aligned} R_1 &= P_1Q_3 - Q_1Q_4 & R_4 &= P_8Q_3 - P_7Q_4 \\ R_2 &= Q_2Q_3 - Q_1Q_5 & R_5 &= -Q_5P_7 \\ R_3 &= P_6Q_3 - Q_1Q_6 & R_6 &= -Q_6P_7 \end{aligned} \tag{2.15}$$

where;

$$\begin{aligned} Q_1 &= P_3 - P_1 & Q_4 &= P_4P_1 - P_3P_2 \\ Q_2 &= P_5 - P_1 & Q_5 &= P_6P_2 + P_1P_5 - P_2^2 - P_1^2 \\ Q_3 &= P_1P_2 + P_1P_3 - P_2^2 - P_1^2 & Q_6 &= P_4P_6 - P_5P_2 \end{aligned} \tag{2.16}$$

where;

$$\begin{aligned} P_1 &= -cos\phi_1 & P_6 &= sin\phi_3 \\ P_2 &= sin\phi_1 & P_7 &= x_g sin\phi_2 - y_g cos\phi_2 + r \\ P_3 &= -cos\phi_2 & P_8 &= x_g cos\phi_2 + y_g sin\phi_2 \\ P_4 &= sin\phi_2 & P_9 &= x_g sin\phi_3 - y_g cos\phi_3 + r \\ P_5 &= -cos\phi_3 & P_{10} &= x_g cos\phi_3 + y_g sin\phi_3 \end{aligned} \tag{2.17}$$

Substituting for all of the parameter values would yield expressions for the six internal contact force components in terms of: r, ϕ_1, ϕ_2, ϕ_3, x_g, y_g, and m_g. Therefore, given an object with a certain radius, three known contact points, and a prescribed internal grasp force focus location and magnitude, a unique solution for the internal grasp forces is obtained by using the above equations. It is apparent that any calculations involved are best left to a computer.

2.7 Constraints on Total Contact Forces

The complete solution for the contact forces is simply the vector sum of the particular and homogeneous contact forces as shown in Equation 2.2. This yields six components of

force expressed in local coordinates at the contact points;

$$\text{contact \# 1:} \qquad \begin{aligned} x_{1_T} &= x_{1_P} + x_{1_c} \\ z_{1_T} &= z_{1_c} \end{aligned} \tag{2.18}$$

$$\text{contact \# 2:} \qquad \begin{aligned} x_{2_T} &= x_{2_P} + x_{2_c} \\ z_{2_T} &= z_{2_c} \end{aligned} \tag{2.19}$$

$$\text{contact \# 3:} \qquad \begin{aligned} x_{3_T} &= x_{3_P} + x_{3_c} \\ z_{3_T} &= z_{3_c} \end{aligned} \tag{2.20}$$

where the "T" subscript denotes total contact force components. The total contact forces must be constrained to produce a stable grasp.

Grasp stability has been widely addressed in robotics literature. This project employs two criteria for maintaining grasp stability. The first is that the manipulator cannot break contact with the object [10:1368]. The second criteria is that the tangential contact forces must be less than the maximum forces sustainable by static friction [4:206]. Given these criteria it is posible to impose requirements on the total contact forces given in Equations 2.18–2.20.

The first requirement is that the normal contact forces be positive. The UMDH finger possesses no means to exert negative contact forces (i.e. suction devices, adhesive surfaces, etc.) Thus, the only way to avoid breaking contact is to maintain positive normal contact forces. This dictates that z_{1_T}, z_{2_T}, and z_{3_T} be positive.

The second requirement is that there be no slip at the contact points. Assuming that static friction at the contact points is the only mechanism available to prevent slip, this requirement will impose conditions on the relative magnitudes of the normal and tangential forces. A static friction "cone" can be defined at each contact point by an angle, θ_s. This angle depends on the coefficient of static friction, μ, which is determined by the maximum ratio of tangential to normal forces before slip occurs.

$$\theta_s = tan^{-1}\mu = tan^{-1}\left(\frac{x_{i_T}}{z_{i_T}}\right)_{max} \tag{2.21}$$

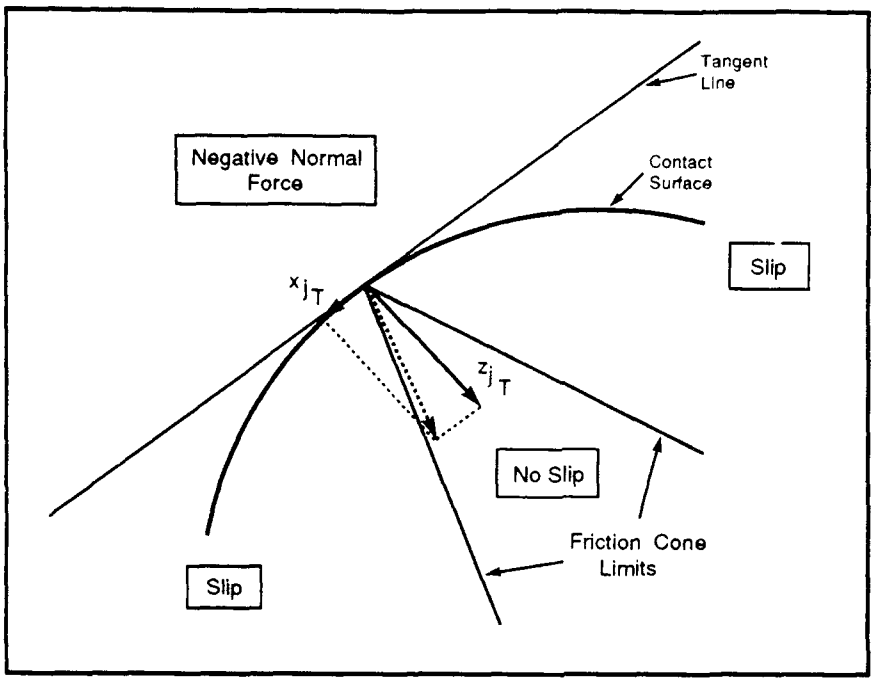

Figure 2.3. Static Friction Cone

Simply stated, the net contact force at each contact point must lie within the friction cone for that contact point, as shown in Figure 2.3.

Three types of contacts result from the two requirements mentioned above, as indicated in Table 2.1. Contact type 3 is undesireable since the normal force is not positive. Contact type 2 is undesireable since the contact would slip. Only contact type 1 meets both requirements. Thus a desireable solution for the contact forces would result in contact type "1" at each contact point. In general, each contact point will have a different contact type. The contact types for the three contact points can be arranged sequentially in a three-digit code such as "312". The first digit of the code is the contact type at contact point number one, etc. Brock uses a similar coding scheme in [2].

2.8 The Constraint Map

Equations 2.6- 2.7, 2.11- 2.17, and 2.18- 2.20 indicate that if the grasp geometry, object radius, and external moment are kept constant, then the only way to alter the contact force solution is to vary m_{ij} or the grasp force focus location, (x_{ij}, y_{ij}). Assuming

Table 2.1. Contact Type Designations

condition	*contact "type"*
$z_{jI} \leq 0$	3
$z_{jI} > 0, x_{jI} \geq \mu z_{jI}$	2
$z_{jI} > 0, x_{jI} < \mu z_{jI}$	1

the friction coefficient stays constant, Table 2.1 reveals that the only way to alter the contact code is to change m_g or (x_g, y_g).

A given manipulator is capable of exerting a finite amount of force on a grasped object (see Section 2.9 for details). This will put a limit on the amount m_g can be increased before the manipulator's capabilities are exceeded. Assuming the value of m_g is at, or close to, that limit, the only remaining option for altering the contact code is to change the grasp force focus location.

Placing the focus at a certain location results in a contact code that can be associated with that particular point. If every point in the grasp plane is tested to see what code is generated, then there will be areas of like codes with well defined boundaries between those areas. The map that shows these boundaries is called the contact code boundary constraint map, which will be referred to as "the constraint map", or "the boundary map".

Since the grasp plane stretches to infinity it is more practical to look at just the part of the plane that is near the grasped object. Even a finite area consists of infinitely many points, so it is also necessary to look at selected points that are evenly spaced. The constraint map will indicate which grasp plane areas have the desireable "111" contact code.

Note that only the position of the grasp force focus varies within each constraint map. All of the other variables (ϕ_1, ϕ_2, ϕ_3, r, m_z, μ, m_g) remain constant. Changing any one of the other variables will result in a different map being generated. Chapter III discusses the development of the computer program that was written to generate constraint maps for this project, and also shows some sample outputs. The constraint map is the primary tool used to determine where the grasp force focus should be placed in various circumstances.

2.9 *Required Joint Torques for Power Grasp*

A constraint map shows where the grasp force focus should be placed in order to have a stable (no slip) grasp. Up until this point, however, the ability of the manipulator to apply the commanded contact forces has not been addressed. Since changing the location of the grasp force focus changes the commanded contact forces, it is likely that locating the focus at some places on the grasp plane will result in commanded contact forces that the manipulator is unable to apply. These are regions which must be avoided.

At each point on the grasp plane the joint torques required of the manipulator (to exert the contact forces which would place the focus at that point) must be calculated, and then compared to the torque limits of the manipulator. This will reveal where on the grasp plane the focus is prevented from being located, and will also show where the "safe" areas are.

The joint torques required will depend not only on the commanded contact forces, but also on kinematic structure of the manipulator and the grasp configuration used. Therefore, from this point forward, the analysis will focus on the manipulator and grasp chosen for this project (the UMDH finger employing a single-finger power grasp).

2.9.1 Notation and Grasp Configuration. The notation that is used for this project is similar to the Denavit-Hartenberg notation [7], and is shown in Figure 2.2. The ith coordinate frame is located at joint $i + 1$ and stays fixed to link i. The 0th frame stays fixed in "world space", and is rotated 90^o with respect to the "object" frame previously shown in Figure 2.1. Due to finger thicknesses additional angles (θ_I, θ_{II}, and θ_{III}) and lengths (a_1, a_2, and a_3) are required to specify the positions of the contact points on each link. Another angle, γ, is needed at the last contact point because the tangential direction at contact point #3 does not always line up with the mid-line of link three. Notice that for contact points #1 and #2 the tangential directions are always aligned with the mid-lines (dashed lines connecting joint centers) of the link making contact.

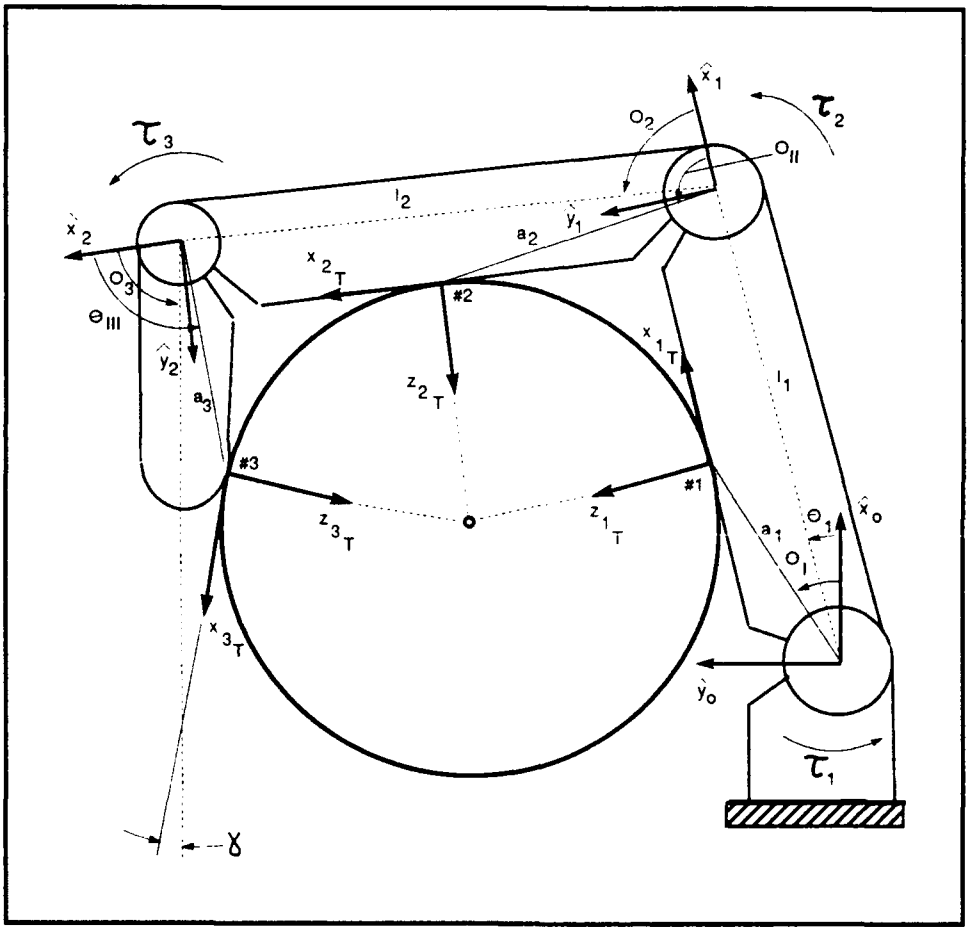

Figure 2.4. Manipulator and Grasp Notation

2.9.2 Manipulator Jacobian. The joint torques required to oppose a certain force on the endpoint of a manipulator are found by using the transpose of the Jacobian matrix [1];

$$\bar{\tau} = J^{t} \bar{F}_{(o)} \tag{2.22}$$

where $\bar{\tau}$ is a vector of the three joint torques, and $\bar{F}_{(o)}$ is a vector of the components of the endpoint force expressed in the (o) frame. J is, in this case, a 2 $\times$ 3 matrix relating infinitesimal joint displacements $d\bar{q}$ to infinitesimal endpoint displacements $d\bar{p}$ [1];

$$d\bar{p} = J d\bar{q} \tag{2.23}$$

where;

$$d\bar{p} = \begin{pmatrix} dx_{(o)} \\ dy_{(o)} \end{pmatrix} \qquad \text{and} \qquad d\bar{q} = \begin{pmatrix} d\theta_1 \\ d\theta_2 \\ d\theta_3 \end{pmatrix} \tag{2.24}$$

Since we are interested in forces at the contact points as opposed to forces at the endpoint of the finger, a Jacobian matrix must be derived for each contact point. These three new Jacobian matrices (J_1^T, J_2^T, and J_3^T) relate infinitesimal joint displacements to the infinitesimal position displacements at the three contact points, respectively.

The force components that are readily available are the x_{jT} and z_{jT} components which are expressed in local coordinates. These components can be assembled into the following vectors;

$$\bar{F}_1 = \begin{pmatrix} x_{1T} \\ z_{1T} \end{pmatrix} \quad \bar{F}_2 = \begin{pmatrix} x_{2T} \\ z_{2T} \end{pmatrix} \quad \bar{F}_3 = \begin{pmatrix} x_{3T} \\ z_{3T} \end{pmatrix} \tag{2.25}$$

These forces are translated into (o) frame components with rotation matrices.

$$\bar{F}_{1(o)} = R_1 \bar{F}_1 \qquad \bar{F}_{2(o)} = R_2 F_2 \qquad \bar{F}_{3(o)} = R_3 \bar{F}_3 \tag{2.26}$$

If contact forces *only* exist at contact #1, then the required joint torques are given by;

$$\bar{\tau} = J_1^T R_1 F_1 \tag{2.27}$$

or, with the matrices inserted;

$$\begin{pmatrix} \tau_1 \\ \tau_2 \\ \tau_3 \end{pmatrix} = \begin{bmatrix} -a_1 s_1 & -a_1 c_1 \\ 0 & 0 \\ 0 & 0 \end{bmatrix} \begin{bmatrix} c_1 & -s_1 \\ s_1 & c_1 \end{bmatrix} \begin{pmatrix} x_{1_I} \\ z_{1_I} \end{pmatrix} \tag{2.28}$$

The shorthand notation of s_I for $sin\theta_I$, etc. is used here.

Similarly, if contact forces only exist at contact #2 then the required torques would be;

$$\bar{\tau} = J_2^I R_2 \bar{F}_2 \tag{2.29}$$

or;

$$\begin{pmatrix} \tau_1 \\ \tau_2 \\ \tau_3 \end{pmatrix} = \begin{bmatrix} -a_2 s_{1II} - l_1 s_1 & a_2 c_{1II} + l_1 c_1 \\ -a_2 s_{1II} & a_2 c_{1II} \\ 0 & 0 \end{bmatrix} \cdot \begin{bmatrix} c_{12} & -s_{12} \\ s_{12} & c_{12} \end{bmatrix} \begin{pmatrix} x_{2_I} \\ z_{2_I} \end{pmatrix} \tag{2.30}$$

where $s_{1II} = sin(\theta_1 + \theta_{II})$, etc.

Finally, if only x_{3_I} and z_{3_I} existed, then the required torques would be;

$$\bar{\tau} = J_3^I R_3 \bar{F}_3 \tag{2.31}$$

or;

$$\begin{pmatrix} \tau_1 \\ \tau_2 \\ \tau_3 \end{pmatrix} = \begin{bmatrix} -a_3 s_{12III} - l_2 s_{12} - l_1 s_1 & a_3 c_{12III} + l_2 c_{12} + l_1 c_1 \\ -a_3 s_{12III} - l_2 s_{12} & a_3 c_{12III} + l_2 c_{12} \\ -a_3 s_{12III} & a_3 c_{12III} \end{bmatrix} \cdot \begin{bmatrix} c_{12III-\gamma} & -s_{12III-\gamma} \\ s_{12III-\gamma} & c_{12III-\gamma} \end{bmatrix} \begin{pmatrix} x_{3_I} \\ z_{3_I} \end{pmatrix} \tag{2.32}$$

where $c_{12III-\gamma} = cos(\theta_1 + \theta_2 + \theta_{III} - \gamma)$ etc.

2.9.3 Multiple Contact Points. For this project, all six contact force components are exerted by the manipulator simultaneously. Therefore, the forces at all three contact points will contribute to the required joint torques. In this situation the total required joint torques are given by;

$$\bar{\tau} = J_1^T R_1 \bar{F}_1 + J_2^T R_2 F_2 + J_3^T R_3 \bar{F}_3 \tag{2.33}$$

which represents the superposition of equations 2.28, 2.30, and 2.32.

The joint torques are now known that would be required to exert the commanded contact forces on the grasped object. These torques can be compared to the maximum joint torque capabilities of the manipulator. However, the UMDH does not have motors at the finger joints, but is tendon driven. Therefore, a translation must be made from maximum tendon tensions to equivalent maximum joint torques.

2.10 Equivalent Maximum Joint Torques

Each link of a UMDH finger is actuated by flexor and extensor tendons. These tendons can be commanded to have a certain "cocontraction" level, causing them to work against each other to provide stiffness to the finger. Assume the cocontraction is set to zero so that the extensor tendons do not work against the flexor tendons. Therefore, only the flexor tendons are in tension when grasping an object. Making this assumption maximizes the manipulator's flexional torque capabilities, and simplifies the calculations needed to find the equivalent maximum joint torques.

The flexor tendon for the third link is attached near the base of the link, and then passes over a pulley located at the third joint. The tendon is routed over guide pulleys in the first and second links, as well as the pulleys at the first and second joints. Tension on the link three flexor tendon will thus cause torques at all three joints. This applies for the link two flexor tendon as well, but it only causes torques at joints one and two. The joint one flexor tendon causes only joint one torques. The amount of torque a certain tendon tension produces depends on the radius of the pulley at the joint in question. All of these factors are reflected in the following equation, which gives equivalent joint torques for a

set of tendon tensions $(T_1\ T_2\ T_3)^T$ [9:p41];

$$\begin{pmatrix} \tau_1 \\ \tau_2 \\ \tau_3 \end{pmatrix} = \begin{bmatrix} r_1 & r_1 & r_1 \\ 0 & r_2 & r_2 \\ 0 & 0 & r_3 \end{bmatrix} \begin{pmatrix} T_1 \\ T_2 \\ T_3 \end{pmatrix} \tag{2.34}$$

where r_1, r_2, and r_3 are the pulley radii at joints one, two, and three respectively. The maximum flexor tendon tensions used for the UMDH finger are derived from values given in [11:p1.13];

$$\begin{pmatrix} T_1 \\ T_2 \\ T_3 \end{pmatrix}_{max} = \begin{pmatrix} 30\,lb_f \\ 20\,lb_f \\ 20\,lb_f \end{pmatrix} = \begin{pmatrix} 133.44\,N \\ 88.96\,N \\ 88.96\,N \end{pmatrix}$$

The pulley radii were measured as $9.5\,mm$, $6.4\,mm$, and $4.8\,mm$ for joints one, two, and three. Using these radii and the above maximum tendon tensions results in Equation 2.34 producing equivalent maximum joint torques of;

$$\begin{pmatrix} \tau_1 \\ \tau_2 \\ \tau_3 \end{pmatrix}_{max} = \begin{pmatrix} 2.958\,Nm \\ 1.139\,Nm \\ 0.427\,Nm \end{pmatrix} \tag{2.35}$$

These torque "limits" are used as the values which are compared against the joint torques needed to produce the desired contact forces, as calculated in Equation 2.33. If any of the needed torques are higher than the corresponding maxima, then the manipulator will not be able to comply. In this case, the grasp force magnitude must be reduced, or the grasp force focus moved to an area of the grasp plane where torque limits are not exceeded. The last statement implies that one knows which areas on the grasp plane are "safe" and which are not. The next section describes how to determine where the safe areas are.

2.11 Joint Torque Constraint Maps

Like the constraint map described in section 2.8, the joint torque constraint map covers an area of the grasp plane near the grasped object and is made up of an evenly spaced grid of test points. The grasp force focus is placed successively at each point, and the torques (needed to exert the contact forces which will place the focus at that point) are calculated and compared with the maximum joint torques found in the previous section. A joint torque constraint map is thus constructed for each of the three joints. The constraint map for joint one shows where on the grasp plane the joint one torque limits are exceeded. The same is true for the joint two and joint three constraint maps.

The UMDH finger is incapable of exerting negative normal forces. For this reason the joint torques required to exert the contact forces are not calculated in areas of the grasp plane where *any* of the three normal forces is negative. This is true whenever the contact code contains the digit "3". Essentially, these areas are ignored when generating the joint torque constraint maps.

Now there are two different constraint map types for each unique set of ϕ_1, ϕ_2, ϕ_3, r, m_y, m_z, and μ values. One type shows where the boundaries are between the areas of different contact codes, and the other shows where torque limits are exceeded. The computer program will generate data for a "stable" map which shows where the "111" contact codes are, and also a "safe and stable" map which identifies the areas of the grasp plane that have "111" codes *and* do not violate any torque constraints. Thus, there are four different types of mappings.

III. Computer Generation of Constraint Maps

The "experimental set-up" for this project consists of a VAX computer running a Fortran program, the listing for which is in Appendix B. The purpose of the program is to generate data files required to plot the four previously defined constraint maps.

There are two types of inputs to the program: those that are prompted for (run specific inputs), and those read from a data file called HAND. DAT (grasp/manipulator specific inputs). The prompted inputs are listed in Table 3.1 along with the nominal values, or ranges of values, used in this study. A description of these inputs follows:

- **External Moment** The moment, in Nm, exerted on the cylindrical object about its z-axis (see Figure 2.1).
- **Grasp Force Magnitude** The sum of the magnitudes, in Newtons, of the internal contact forces. Set by the user, and defined in Equation 2.8.
- **Friction Coefficient** Coefficient of static friction between the object and the manipulator. The same value is used at all three contact points.
- **Map Scale** The number of cylinder radii from the center of the map to its edge.
- **Resolutions** The number of pixels to be used as test points (focus locations) in the x and y directions. The total number of test points in the "grid" is RESX $\times$ RESY.
- **Cylinder Radius** The radius of the cylinder in meters.
- **Contact Positions** The contact positions, measured counterclockwise from the "up" position on the cylinder, in degrees (see Figure 2.1). Note that a notational singularity exists for $\phi_1 = 0^o$. This results from a $sin\phi_1$ in the denominator of the expression for z_{l_1} (see Equations 2.11).
- **Search Querry** Asks if the user desires the extra resolution that can result from searching for contact code boundaries not only from left-to-right, but from top-to-bottom as well. This extra resolution affects only the boundary constraint map.
- **Run Number** A two-digit number appended to filenames of output data files in order to identify which run produced that file.

Table 3.1. Prompted Inputs for Fortran Program

Input	*Variable Name*	*Nominal Values*
1. External Moment	MZ	0–.25 Nm
2. Grasp Force Magnitude	MG	16–230 N
3. Friction Coefficient	MU	.3–.8
4. Map Scale	S	1.5
5. X-resolution	RESX	200
6. Y-resolution	RESY	200
7. Cylinder Radius	R	.009–.030m
8. Contact Positions	PHI1, PHI2, PHI3	Various
9. Top-to-bottom Search?	ANS	Y
10. Two-digit Run Number	RUN	User Option

The data file input values are dependent on the specific grasp geometry and manipulator employed. These factors are taken into account only for the power grasp case. The required inputs are listed in Table 3.2, and are self-explanatory. Values used for these inputs are further discussed in Section 3.2.3.

After all prompted and data file values are input, the particular solution for the contact forces is calculated using Equations 2.6–2.7. Before entering the main iteration loop the elements for the matrices in Equations 2.27–2.32 are calculated.

The main iteration loop is run once for each pixel of the constraint map(s). The starting point is the top, left corner of the map. The internal contact forces required to locate the grasp force focus at that point are then calculated, and added to the particular solution for the contact forces, as per Equations 2.18–2.20. A contact code is then generated for that pixel according to the criteria in Table 2.1, and the required joint torques are also calculated. If any of the three required joint torques are above their corresponding maxima, then a data point (the pixel coordinates) is sent to the output data file containing violation points for that particular joint. There are three such data files; one for each of the three joints.

The contact code for this first pixel is kept in memory, and the next iteration loop is started. The next pixel analyzed is the one to the right. Once again, internal contact forces are calculated and added to the particular solution to get the total contact forces.

Table 3.2. Data Inputs for Fortran Program

	Input	*Variable Name*
1.	Link 1,2 length	L1,L2
2.	Distance from Jt.1,(2,3) to contact#1,(#2,#3)	A1,(A2,A3)
3.	Joint 1 displacement	THETA1
4.	Joint 2 displacement	THETA2
5.	Joint 3 displacement	THETA3
6.	$\theta_{I,II,III}$ (see fig. 2.4)	THI,THII,THIII
7.	γ (see fig. 2.4)	GAMMA
8.	Joint 1 maximum torque	TAU1MAX
9.	Joint 2 maximum torque	TAU2MAX
10.	Joint 3 maximum torque	TAU3MAX

These are again analyzed and a contact code is generated. If this code is *different* from the code of the previous pixel, then a boundary between areas of like contact codes has been found. This causes a data point (midway between the pixels) to be output to the contact code boundary constraint map data file. If the contact code is the same as that of the previous pixel, then there is no boundary, and no data point is output.

The program proceeds in this way from left to right, examining one row at a time. Notice that if a boundary between two different contact code areas is a horizontal line, then the routine described above will not find it. This is where the top-to-bottom boundary search is useful. A "y" response to the top-to-bottom search querry will cause the computer to search through the grasp plane twice. After completing the normal program routine, a second iteration loop reviews the codes in a top-to-bottom manner looking for boundaries that would otherwise not show up.

There are a total of seven output data files generated for each run of the program. If ## is the two-digit run number input by the user, then the output files are;

- BNDRY##. DAT : Data points corresponding to boundaries between different contact code areas.
- STABLE##. DAT : Data points where the contact code is "111".
- CNTCTS##. DAT : A file of three data points indicating where the contact points are on the cylinder.
- JTONE##. DAT : Data points where joint one torque limits are exceeded.
- JTTWO##. DAT : Data points where joint two torque limits are exceeded.
- JTTHR##. DAT : Data points where joint three torque limits are exceeded.
- SAS##. DAT : "Safe and stable" data points that have "111" contact codes and do not exceed any torque limits.

3.1 Example Constraint Maps.

Two types of grasps are mapped using the program described above. The first consists of fingertip grasps (i.e. using three fingers to grasp the cylinder in a cross-sectional plane). The second type is a chosen single-finger power grasp with one contact for each of the three links of the finger.

Fingertip grasps are examined in order to explore the behavior of the boundary constraint map to changes in input variables. Joint torque limits are not considered in these cases. Once the behavior of the boundary constraint map is examined and understood, the method is applied to the specific single-finger power grasp chosen for this project. Joint torque limits can be examined for the single-finger grasp since the manipulator dimensions and grasp geometry are known.

Figure 3.1 shows an example of a fingertip grasp boundary constraint map. The use of three independent fingers allows many possible grasp geometries, one of which is the symmetric grasp shown. The grasp is called "symmetric" due to the even spacing of the

contact points. The desireable contact code "111" is produced if the grasp force focus is placed in the stable (shaded) area at the center of the cylinder. For this particular map the external moment m_z was set to zero, resulting in straight boundary lines. The friction cones can be clearly seen extending from the contact points, and are part of the boundary set, as expected. The cones extend in both directions since it is possible for the grasp force focus to be outside the cylinder. However, the stable area is restricted to the area inside *all three* friction cones.

Figures 3.2–3.4 show an example of a set of constraint maps generated for the chosen single-finger power grasp. The external moment has been set to an arbitrary positive value causing several boundary lines to curve. Once again the desireable stable area is identified by the shaded region of the map. Figures 3.3 and 3.4 show the "unsafe" areas on the grasp plane where joint torque limits are exceeded for joints two and three. Joint three torques are exceeded throughout the stable area shown in Figure 3.2. Note that the clear areas outside the contact triangle are not necessarily areas where torque violations do not occur. The majority of the areas outside the contact triangle contain a "3" somewhere in the contact code. Such areas are not tested for torque limit violations, as explained in Section 2.11. For this example there are no "safe and stable" areas due to the extent of the joint three torque violations.

3.2 Additional Considerations

3.2.1 Slip at a Single Contact Point. There may be useful areas on the grasp plane just outside of the stable area. Generally, crossing a boundary line on the boundary map indicates that one digit of the contact code has changed. Therefore there are areas next to the stable area where the contact code is "211", "121", or "112" indicating that the grasp is slipping at only one of the contact points. Are these useful grasps?

An important point to note is that the contact code is only accurate for the initial application of the grasp. If one of the contact points slips after the grasp is first applied, then the friction at that contact point is dynamic, not static. Dynamic friction forces are generally lower in magnitude than static friction forces, and the contact point that is slipping is now less capable of helping to counter the applied external moment. In order

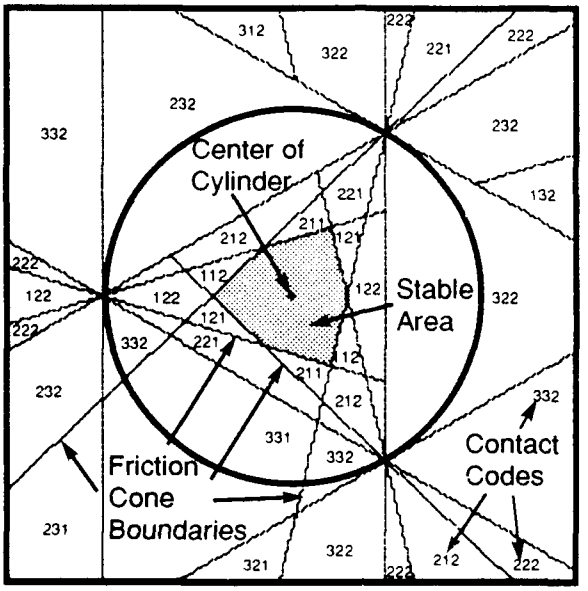

Figure 3.1. Example Constraint Map: Fingertip Grasp

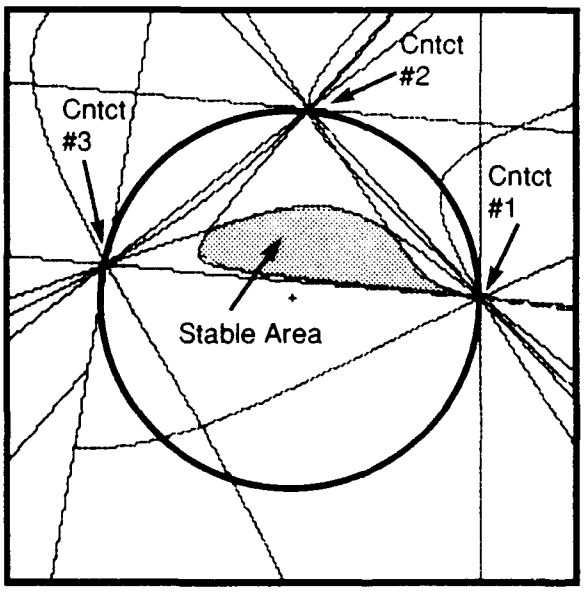

Figure 3.2. Example Constraint Map: Power Grasp

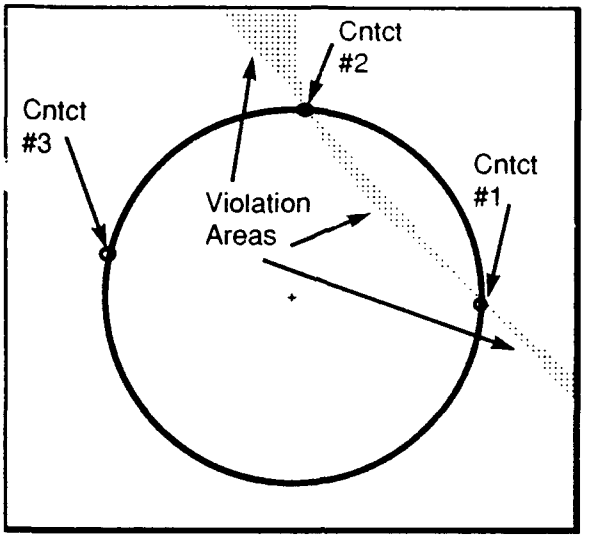

Figure 3.3. Joint Two Torque Violations

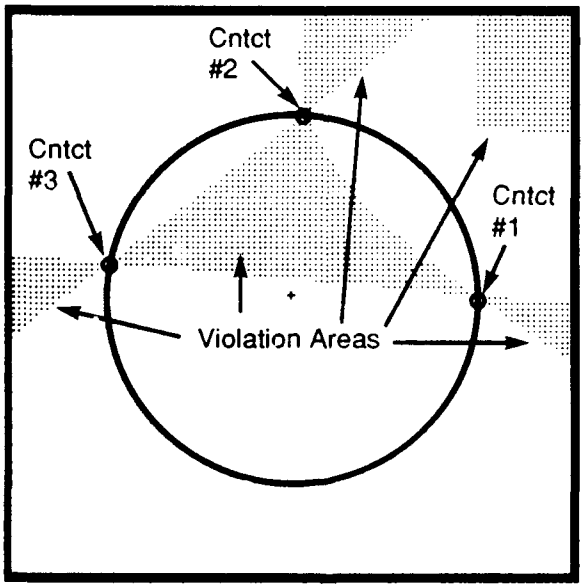

Figure 3.4. Joint Three Torque Violations

for the grasp to be maintained the other two contact points will have to "do more work". This extra burden may induce slipping at one or both of the other two contact points.

Another complication involved in analyzing this dynamic case is that the grasp geometry is changing. If one of the contact points slips, the manipulator will move into a new geometry which changes the ability of the manipulator to exert grasp forces. This project does not deal with these complications, and therefore only areas with contact codes "111" will be considered acceptable for focus locations.

3.2.2 Sign of z_{3_i}. Examining Figure 3.1 reveals that the map is not completely symmetrical, as would be expected for a symmetrical grasp. Some of the friction cone lines disappear and then reappear. The reason for this is found in Equations 2.11 which yield the solution for the internal contact forces. Inspection of the first equation reveals that it is impossible for z_{3_i} to have a negative value, since m_{ij} must be positive. The result is that the third contact point's normal contact force will always be positive, and thus there will never be a "3" as the third digit of the contact code. In Figure 3.1 this results in a mirror image of the boundary lines about a line normal to the cylinder surface at the third contact point, located at the upper right portion of the cylinder.

The only portions of the map that are affected by the asymmetry are those that are outside the triangle made by the three contact points. This premise was tested by rewriting the program and forcing z_{2_i} to be positive. Numerous different situations were tested to see if the stable areas were any different on the two sets of maps generated. There were no differences in the stable areas even when they were outside the contact triangle, a possibility that will be discussed later. The conclusion is that forcing z_{3_i} to be positive has no affect on the location or shape of the stable areas.

3.2.3 Choice of Grasp and Uniqueness. Various three-finger grasps are used in this project to show how the constraint map behaves for a wide range of input variables. Once this behavior is understood, the grasp force focus placement method is applied to a specific single-finger power grasp (a simplification of the full hand power grasp). The reasoning behind the grasp choice, and the exact parameters of the grasp, are presented here.

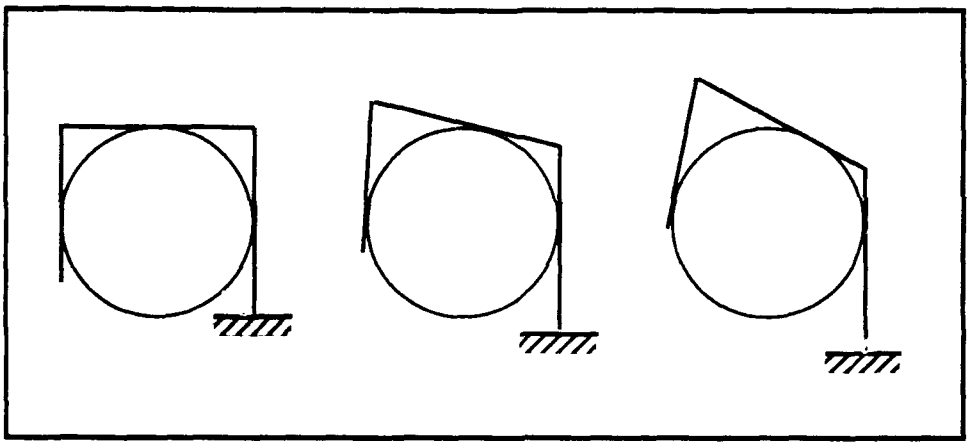

Figure 3.5. Possible Grasps of a Fixed Radius Cylinder

Joints two and three of the UMDH finger are both limited to 90° of bend, preventing the finger from wrapping around an object more than 180°. The finger could have contacts that are 180° apart if grasping an $8mm$ radius cylinder. However, this grasp causes the finger links to touch each other, causing the contact forces to be reduced. Using a $9mm$ radius cylinder eliminates the finger link interference, and allows for a grasp that wraps 170° around the perimeter.

Simply designating the cylinder size does not uniquely determine the grasp configuration. Figure 3.5 shows a three link finger with different grasp configurations on a single cylinder. What one still needs to be specify is where the contact point will be on any one of the three UMDH finger links. Designating the contact location on one finger will determine the other two contact locations due to the fixed dimensions of the links. It is assumed that neither the cylinder nor the links deform when in contact.

So, two variable values must be specified for the grasp to be unique; 1) the cylinder radius, and 2) the contact location on one of the links. In order to determine contact locations for this project the chosen cylinder was placed in a UMDH single-finger power grasp similar to the leftmost diagram in figure 3.5. The needed angles and distances were measured and placed in the HAND.DAT data file. The values are listed here in Table 3.3 (see figure 2.4 for variable definitions), and are not varied in this study.

The constraint map generation program can now be used to analyze constraint map

Table 3.3. HAND.DAT Values

Angle	*Value(Deg)*	*Distance*	*Value(mm)*
θ_1	0	l_1	44
θ_2	85	l_2	33
θ_3	75	a_1	26
θ_I	25	a_2	22
θ_{II}	112	a_3	18
θ_{III}	101.4		
γ	10		

behavior, and to determine how the grasp force focus should be placed in order to enhance the torque resistance capability of the chosen grasp.

IV. Results and Discussion

In order to explore what happens to the constraint maps as variables change, the most simple situation is explored first and complications are introduced one at a time. The fingertip grasp is explored in depth, starting with symmetric grasps and varying only one input variable at a time. Next, multiple variables are changed simultaneously in order to find patterns of map behavior. The effect of using asymmetrical contact points is examined by looking at three categories of grasp geometries, including: "enveloping", "opposing", and "non-enveloping". Finally, the single-finger power grasp is examined which requires that joint torque constraints be taken into account. The specific power grasp employed is as described in Section 3.2.3, which is a non-enveloping grasp within the capabilities of the UMDH finger.

4.1 Symmetric Fingertip Grasps

All of the symmetric fingertip grasps tested here use contact points at 90^o, 210^o, and 330^o (measured counterclockwise from vertical). Input variables will be changed one at a time, and then together, to see how they affect the boundary constraint map.

4.1.1 Effects of Single Variable Changes.

4.1.1.1 Coefficient of Friction. A very simple case is examined first. The external moment on the cylinder is set to zero, the internal grasp force magnitude is set to an arbitrary positive value of $100N$, and the radius of the cylinder is $9mm$. The starting value for the coefficient of friction, μ, is .3 which results in the map shown in Figure 4.1 where the friction cones are inside the triangle formed by the three contact points. In Figure 4.2 μ has been increased to .5 and the friction cones are getting larger, resulting in a larger stable area at the center of the cylinder. In Figure 4.3 μ has been increased to .57.50 ($tan30^o$) so that the friction cones coincide with the lines joining the contact points. This is the simplest map possible, and the stable area is all of the area inside the contact triangle. Next the friction coefficient is increased to .8 which produces the map

in Figure 4.4. Notice that the friction cones are now outside the contact triangle, but the stable area remains limited to the area inside the contact triangle.

4.1.1.2 External Moment. The effects of increased friction are not surprising, and could even be predicted since the friction constraint is applied to the total contact forces. However, increasing the external moment, m_z, affects only the particular portion of the contact force solution, making it difficult to predict what will happen to the constraint map if m_z is set to some nonzero value. That job is left to the computer.

For the next map, Figure 4.5, the same input values are used as in Figure 4.3, except m_z is set to .15 Nm. Therefore all differences between the two maps are due to the nonzero value of m_z. Notice that the stable area becomes more constricted, but is still symmetric about the center of the cylinder, as would be expected for a symmetrical grasp.

Figure 4.6 uses a negative value for m_z, $-.15\ Nm$, which means the torque vector on the cylinder is into the page. The only differences between Figures 4.5 and 4.6 are outside the contact triangle for this symmetric grasp case.

Next, m_z is increased to .4 Nm and .7 Nm in Figures 4.7 and 4.8, respectively. Notice that the stable area shrinks until it disappears at the center of the cylinder at some value of m_z between .4 and .7 Nm. This indicates that for a symmetrical grasp the best place to put the grasp force focus is at the center of the cylinder, since that is the last place that will produce a stable grasp.

4.1.1.3 Internal Grasp Force Magnitude. The next important variable to be examined is the internal grasp force magnitude, m_g. The contact code "222" at the center of Figure 4.8 indicates that the contacts are slipping at all three points. If m_g is increased above a certain point the slipping should stop, and the stable area should return. In Figure 4.9, m_g has been increased to 160 N and the stable area has reappeared. The value of m_g is increased further in Figure 4.10 to 230 N which causes the size of the stable area to further increase.

4.1.1.4 Cylinder Radius. A larger cylinder radius gives the contact forces a larger moment arm with which to resist the external moment, m_z. Therefore, a larger

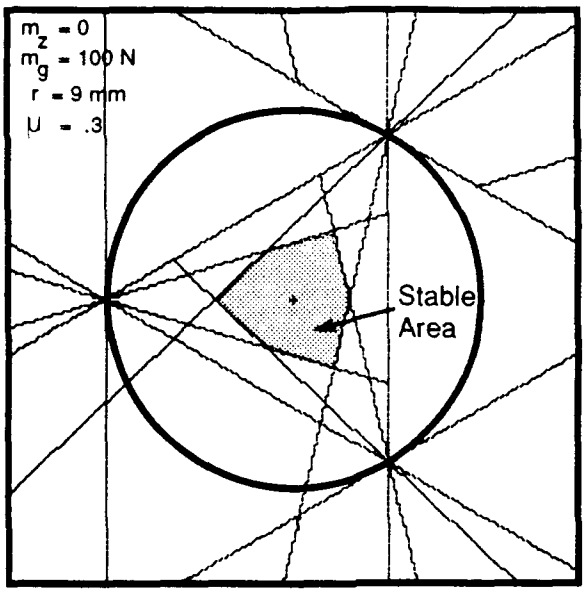

Figure 4.1. Low Friction Coefficient

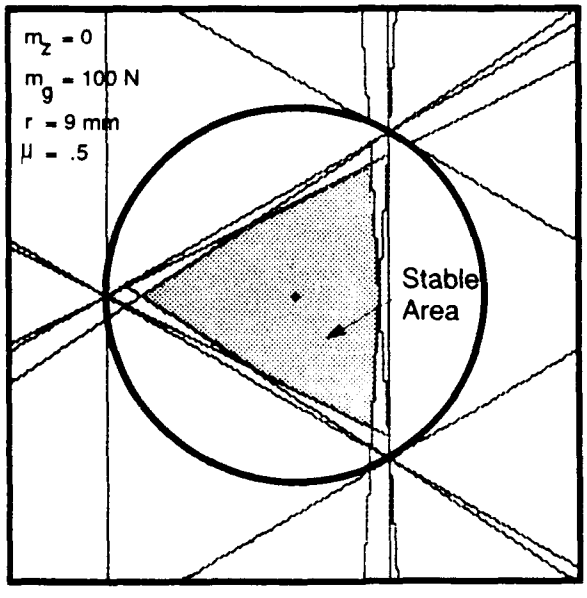

Figure 4.2. Medium Friction Coefficient

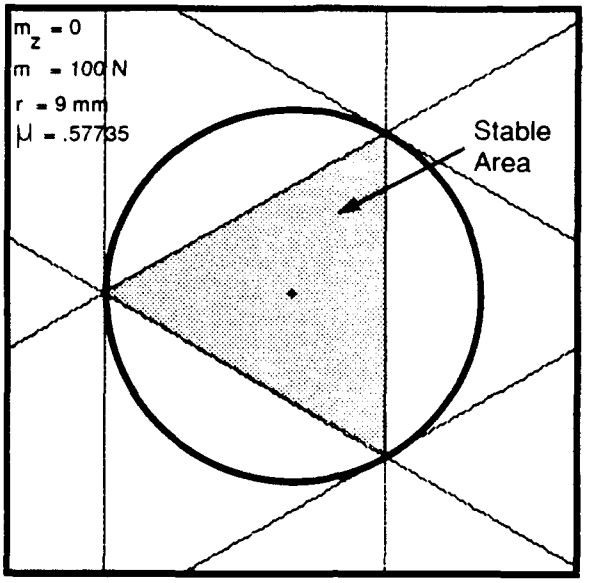

Figure 4.3. $\mu = .57735$

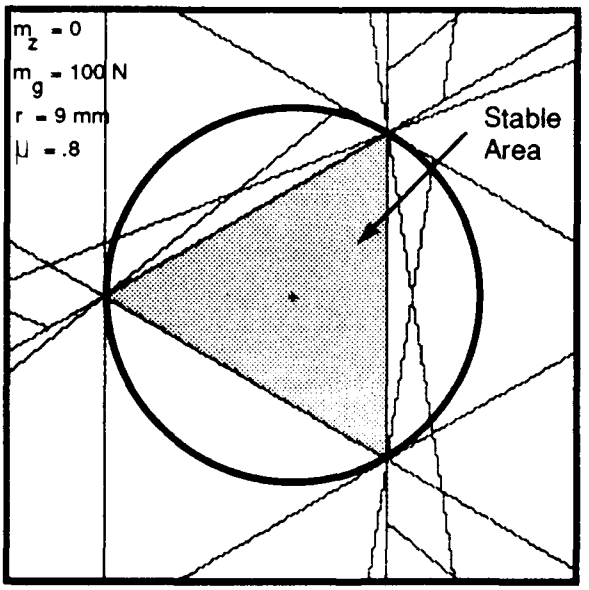

Figure 4.4. High Friction Coefficient

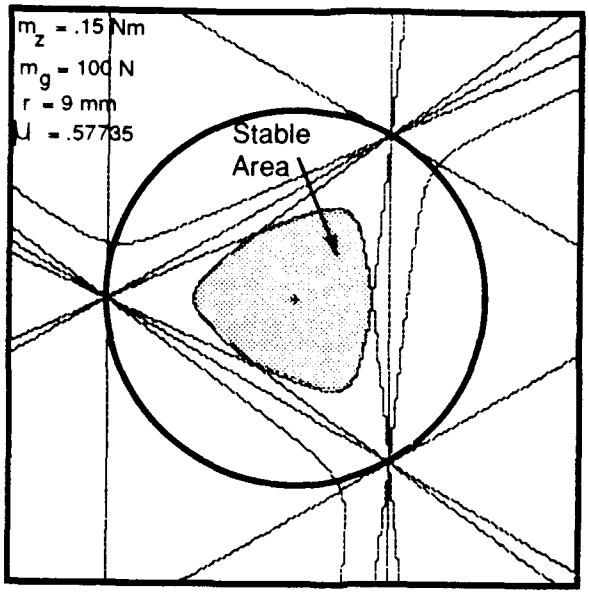

Figure 4.5. Small, Positive m_z

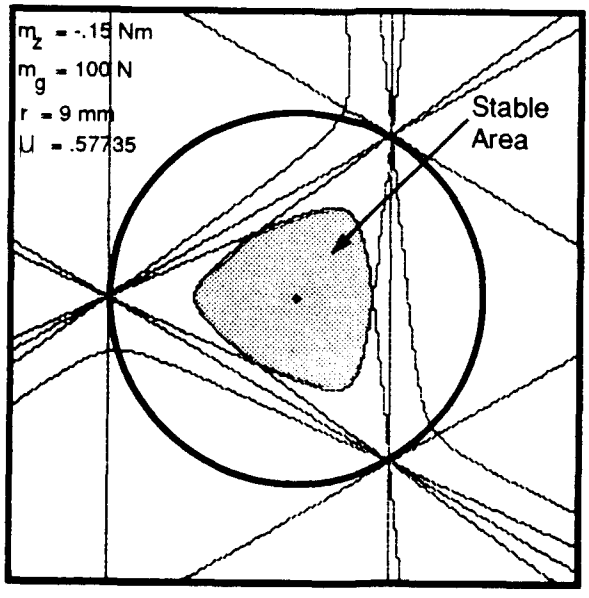

Figure 4.6. Small, Negative m_z

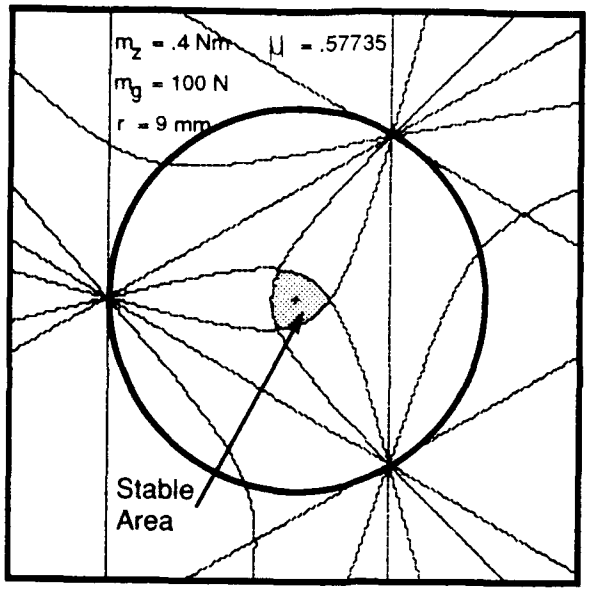

Figure 4.7. Medium, Positive m_z

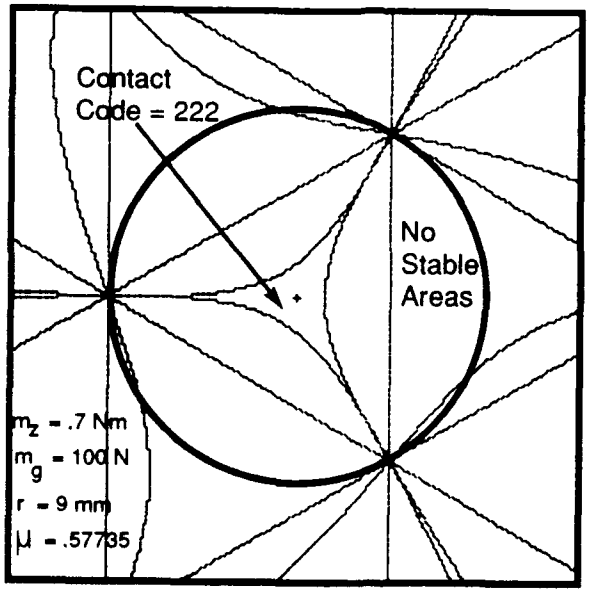

Figure 4.8. Large, Positive m_z

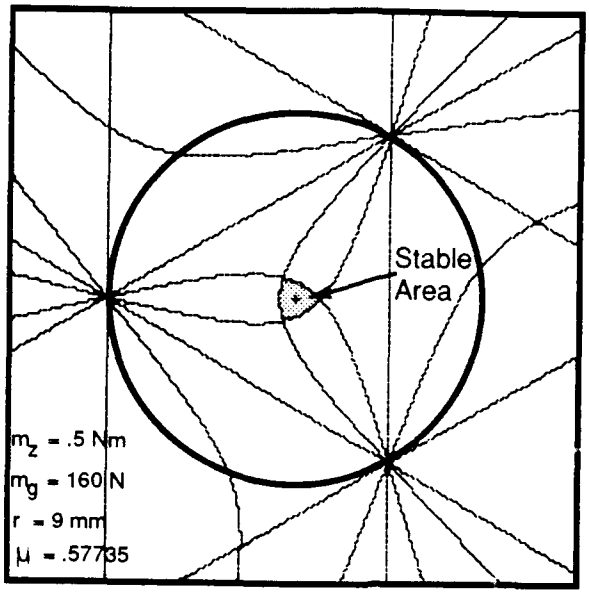

Figure 4.9. Increased m_g

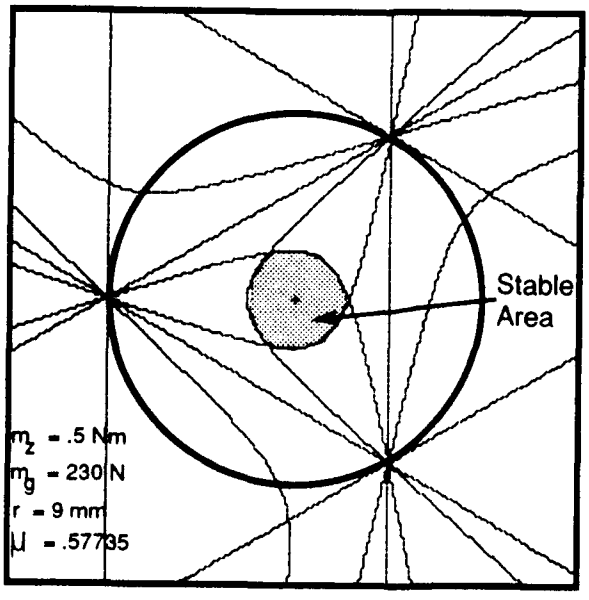

Figure 4.10. Further Increased m_g

cylinder radius results in a larger stable area. Using the values in Figure 4.8 as a starting point again, the cylinder radius, r, is increased to 15 mm in Figure 4.11. This also causes the stable area to reappear, as did increasing m_g. Further increasing r to 30 mm results in the larger stable area seen in Figure 4.12.

4.1.2 Effect of Multiple Variable Changes. Up until now the input variables have been changed one at a time. However, there have been some recognizable patterns as to how each variable affects the constraint map, and these patterns can be used to predict what will happen when multiple variables are changed. For example, increasing either m_g or r tends to increase the size of the stable area, so increasing both of them at once would certainly give a larger stable area. What remains unclear is, what happens if r is increased and m_g is decreased? Similarly, what if both m_g and m_c are increased?

4.1.2.1 A Constant c_{map} Value. Answering the questions above requires a closer look at how the contact forces are calculated, and how the constraints are applied to them.

The positive-normal-force constraint and friction cone constraint are applied to the total contact forces, which are made up of the particular solution contact forces and internal contact forces. Equations 2.6 and 2.7 (the particular solution) can be rewritten as;

$$\begin{aligned} \boldsymbol{x}_{1_p} &= \tfrac{m_c}{r}(EXPR1) \\ \boldsymbol{x}_{2_p} &= \tfrac{m_c}{r}(EXPR2) \\ \boldsymbol{x}_{3_p} &= \tfrac{m_c}{r}(EXPR3) \end{aligned} \tag{4.1}$$

and Equations 2.11–2.17 (the homogeneous solution) can be rewritten as;

$$\begin{aligned} \boldsymbol{x}_{1_i} &= m_g(EXPR4) & z_{1_i} &= m_g(EXPR7) \\ \boldsymbol{x}_{2_i} &= m_g(EXPR5) & z_{2_i} &= m_g(EXPR8) \\ \boldsymbol{x}_{3_i} &= m_g(EXPR6) & z_{3_i} &= m_g(EXPR9) \end{aligned} \tag{4.2}$$

where the "EXPRi" values are functions of the contact locations only, and do not change for a specific grasp of a specific cylinder. The above expressions can be combined for the

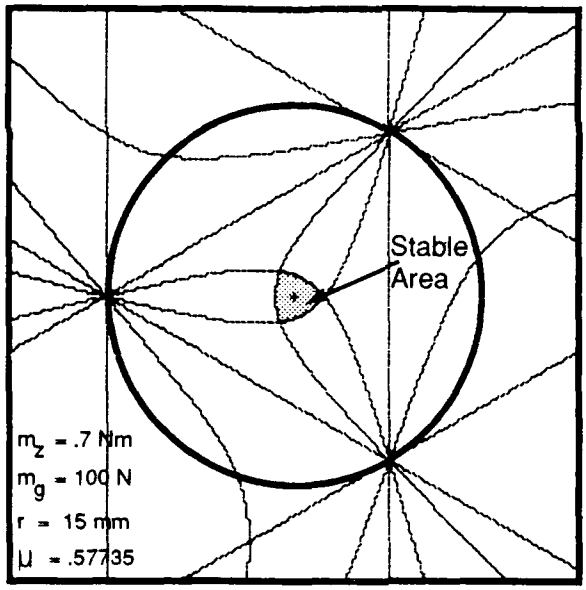

Figure 4.11. Increased r

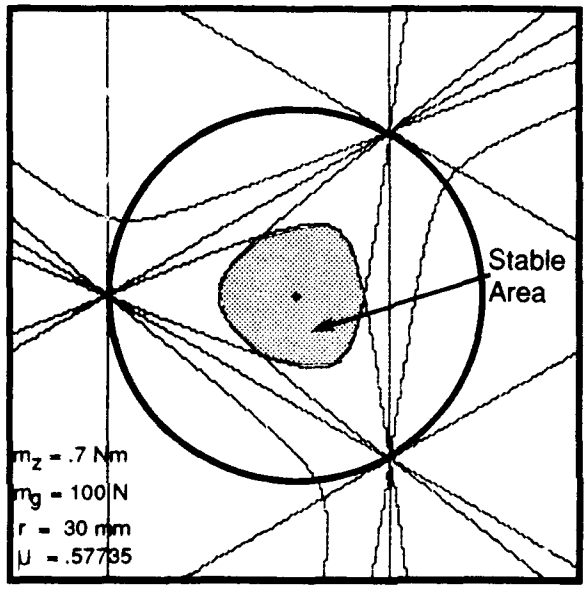

Figure 4.12. Further Increased r

total contact forces;

$$\begin{aligned} x_{1_f} &= \tfrac{m_z}{r}(EXPR1) + m_g(EXPR4) \\ x_{2_f} &= \tfrac{m_z}{r}(EXPR2) + m_g(EXPR5) \\ x_{3_f} &= \tfrac{m_z}{r}(EXPR3) + m_g(EXPR6) \end{aligned} \tag{4.3}$$

$$\begin{aligned} z_{1_f} &= m_g(EXPR7) \\ z_{2_f} &= m_g(EXPR8) \\ z_{3_f} &= m_g(EXPR9) \end{aligned}$$

Now apply the constraints to the total contact forces, using contact #1 as an example. The normal force will be positive if;

$$m_g(EXPR7) > 0 \tag{4.4}$$

As long as the sign of m_g is not changed, this inequality will be unaffected. The friction cone constraint is not violated if;

$$\left|\frac{m_z}{r}(EXPR1) + m_g(EXPR4)\right| < \mu\, m_g(EXPR7) \tag{4.5}$$

or;

$$\left|EXPR1 + \left(\frac{m_g r}{m_z}\right) EXPR4\right| < \mu \left(\frac{m_g r}{m_z}\right) EXPR7 \tag{4.6}$$

or;

$$|EXPR1 + c_{map} EXPR4| < \mu c_{map} EXPR7 \tag{4.7}$$

where;

$$c_{map} \equiv \frac{m_g r}{m_z}$$

The inequality in Equation 4.7 will remain unchanged if the value of c_{map} (which is unitless) remains constant. If both constraint inequalities (Equations 4.4 and 4.7) are unchanged, then the constraint map will always be the same for a specific grasp of a specific object.

The conclusion is that for a particular grasp configuration and friction coefficient,

if m_g is kept positive and c_{map} remains constant, then the constraint map will remain unchanged. So, for example, if m_g is doubled and r is halved, the constraint map will stay the same. Figures 4.12–4.14 demonstrate this conclusion.

Figure 4.12 has input variables which give a c_{map} value of 4.2857. Figure 4.13 below has the same c_{map} value, but uses widely different input variables. The same is true for Figure 4.14. Notice that the maps are identical, as predicted. Since each map can be characterized by a certain c_{map} value, each grasp will have a c_{map} value which represents the point where the stable area disappears. This property will become useful in later analyses.

4.2 Asymmetric Fingertip Grasps

Since symmetric grasps are not always possible, it is valuable to know what happens to the constraint map when asymmetric grasps are used. These are still fingertip grasps, but the configurations have changed.

Asymmetric grasps are divided into three categories. The first includes those grasps where the maximum angular separation between any two adjacent contact points is less than 180°, which will be called "enveloping grasps". The second is where the maximum angular separation is exactly 180°, or "opposing grasps". Finally, the third category is where the maximum angular separation exceeds 180°, which are "non-enveloping grasps".

The main objective for this project is to determine how to maximize the torquing ability of the grasp. The way to accomplish this goal is to place the internal grasp force focus at the point where the stable area disappears as the external torque is increased. This ensures that the focus will remain in the stable area for the longest possible time as the stable area shrinks. When the stable area disappears the capabilities of the grasp have been exceeded.

The approach used in this section is to pick a grasp configuration for each category and increase the external moment until the stable area disappears. This will indicate the most advantageous position for the grasp force focus for each category of grasp.

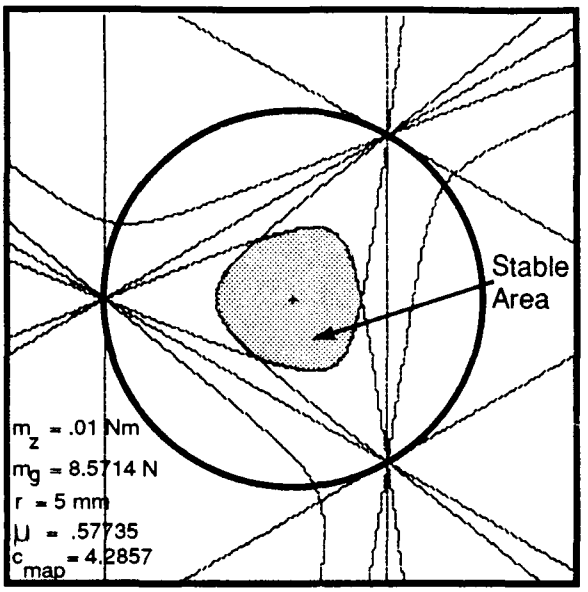

Figure 4.13. Constant c_{map} Demonstration #1

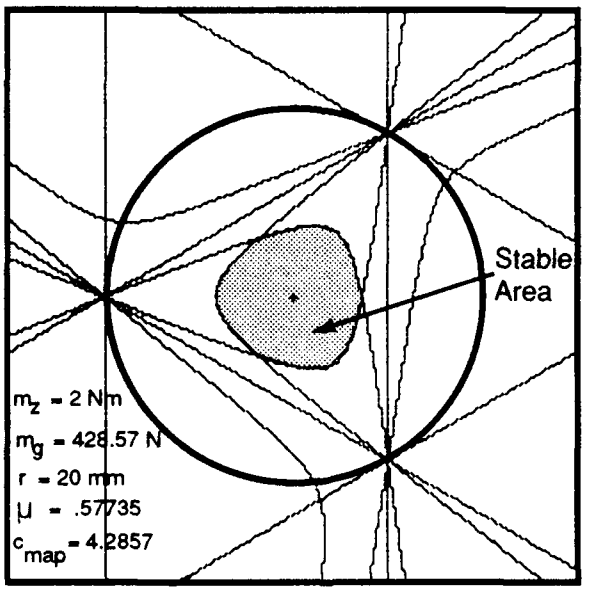

Figure 4.14. Constant c_{map} Demonstration #2

4.2.1 Enveloping Grasps. The grasp configuration chosen for this category has contact locations at 20^o, 90^o, and 230^o, the largest angular separation between contacts being 150^o (i.e. $< 180^o$). The grasp on the $9mm$ radius cylinder will keep a constant internal grasp force magnitude of $60N$ (arbitrary), and a moderate μ value of .8 is used. The map in Figure 4.15 shows that stable areas exist for an external moment value of $.3\,Nm$ (c_{map} value of 1.8).

As Chapter III described, one of the output data files generated by the computer program is a collection of all of the stable points in the area mapped. Figure 4.16 shows a map of the stable areas in Figure 4.15. Notice there are stable points outside the contact triangle. These are valid stable points, although they tend to disappear sooner than the stable area inside the contact triangle for this enveloping grasp case.

In Figure 4.17 the external moment has been increased to $.35\,Nm$ and the stable area has become much smaller. In Figure 4.18 the stable area has almost disappeared with the value of m_z set at $.41\,Nm$. Notice that, for an enveloping grasp, the stable area disappears at the exact center of the cylinder even when the grasp is not symmetric. This is the best location for the grasp force focus if maximum torque resistance is desired. The lowest c_{map} value reached before disappearance is 1.32, which is independent of the choices for m_g and r. For example, if a value of $100\,N$ was used for m_g, and $9\,mm$ for r, the stable area would have disappeared when m_z reached $.682\,Nm$ (i.e. when c_{map} reached 1.32).

4.2.2 Opposing Grasps. The grasp configuration chosen for the opposing grasp category has contacts at 30^o, 100^o, and 280^o. The friction coefficient is kept at .8, and m_g is set at $80\,N$ (arbitrary). This time the starting value for m_z is $.2\,Nm$ ($c_{map} = 3.6$) which produces the map shown in Figure 4.19. The stable areas for this map are as shown in Figure 4.20.

Once again the external moment is increased to see how the stable area behaves. When m_z is increased to $.35\,Nm$ the stable area becomes thinner as shown in Figure 4.21. Increasing m_z further to $.54\,Nm$ seems to indicate that the stable area reduces to a thin line between the opposing contact points before disappearing, as shown in Figure 4.22. Any point on this line is a good location for the grasp force focus. Note that the c_{map}

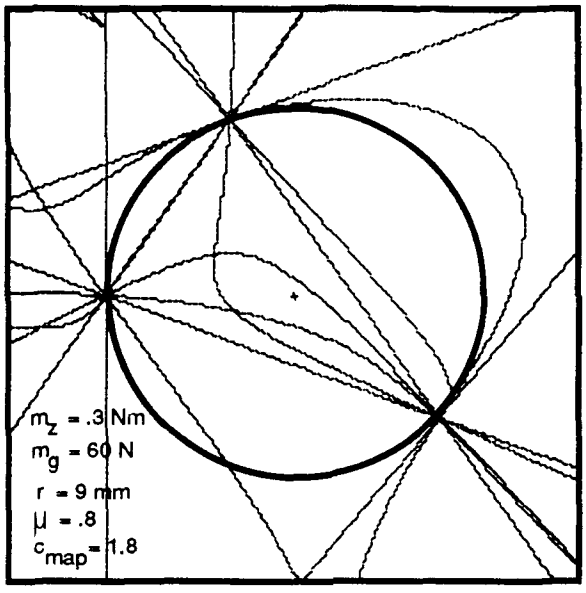

Figure 4.15. Enveloping Grasp Constraint Map

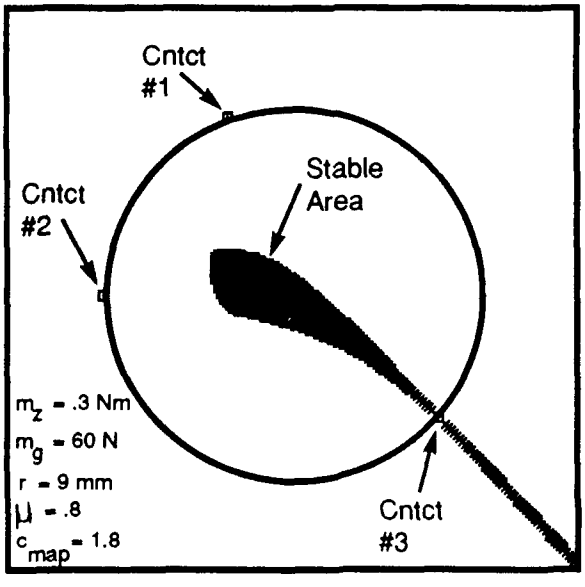

Figure 4.16. Enveloping Grasp Stable Areas (Low m_z)

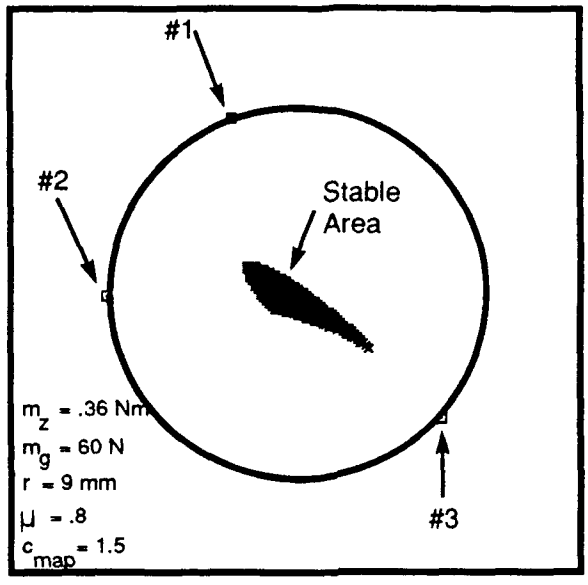

Figure 4.17. Enveloping Grasp Stable Area (Medium m_z)

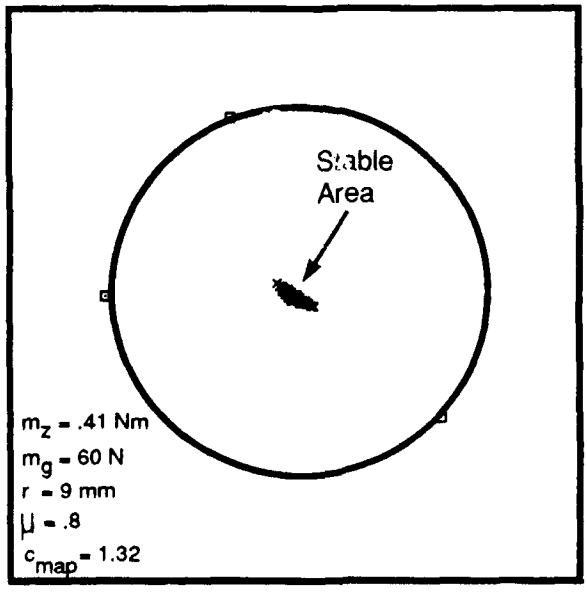

Figure 4.18. Enveloping Grasp Stable Area (High m_z)

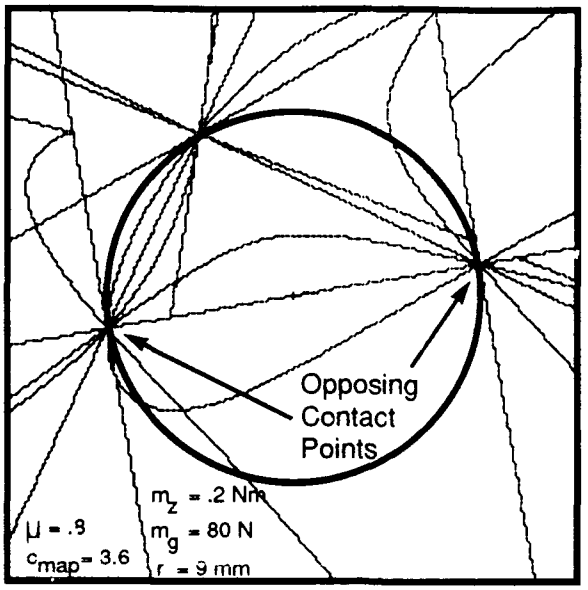

Figure 4.19. Opposing Grasp Constraint Map

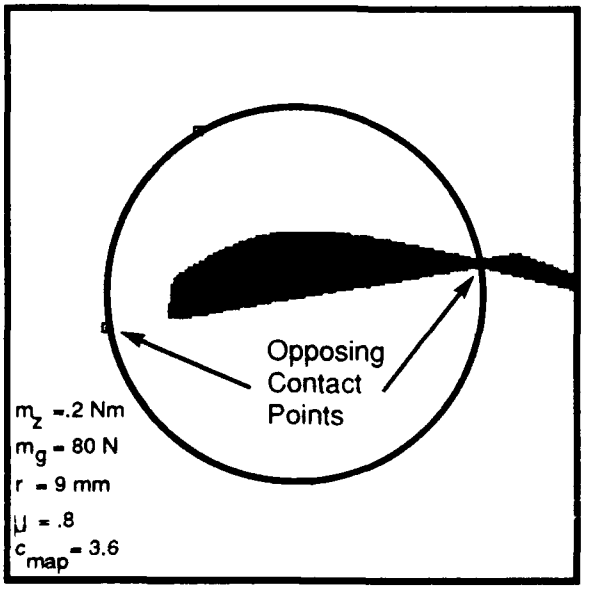

Figure 4.20. Opposing Grasp Stable Areas (Low m_z)

value at disappearance is almost the same as that for the enveloping grasp case.

4.2.3 Non-enveloping Grasps. This last category of asymmetrical fingertip grasps looks at an example which uses contact locations at 210°, 260°, and 330°. This means that there is 240° of angular separation between two of the contact points (i.e. $> 180°$). This grasp is something similar to trying to palm a basketball while someone is twisting the basketball, and so it is expected that only low levels of torque will be tolerable.

The external moment is set to .001 Nm as a starting point (see Figure 4.23), and 100 N is used for m_g. The friction coefficient is kept at .8 . Figure 4.24 shows the stable area for this value of torque. In Figures 4.25 and 4.26 m_z is increased to .04 Nm and .075 Nm, respectively. Notice how the stable area reduces to a short line just outside the bottom contact point. Also notice how the stable area has almost disappeared while c_{map} is still as high as 12. This tells us that for the same amount of internal grasp force magnitude, this grasp is less capable of resisting external torque than the enveloping or opposing grasps, and can be thought of as less "efficient" at resisting external torque. The trend seems to be that further envelopment of the grasped object permits the use of lower c_{map} values before the disappearance of the stable area.

The reason the stable area is located only near the bottom contact point in Figure 4.26 is because of the direction of the torque. However, if the direction of torque is reversed, as in Figure 4.27, the stable area disappears completely. The only possible reason for this happening is the fact that the angular separation between contact points one and two is different than that between two and three. If contact two is moved from 260° to 280°, as in Figure 4.28, the stable area reappears as a "mirror image" of what it was in Figure 4.26.

The upper contact point in Figure 4.28 will be referred to as the "leading contact point", and the others are the "intermediate" and "trailing" contact points. If the torque direction were reversed, as in Figure 4.26, then the bottom contact point would be the leading contact point (use the torque arrow to determine which is which).

The torque resistance capability of the grasp is greater when the intermediate contact point is closer to the leading contact point. Also, as torque is increased the stable area

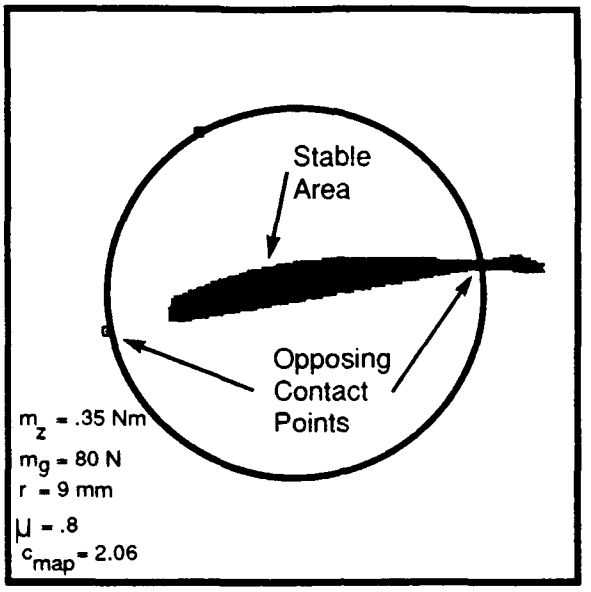

Figure 4.21. Opposing Grasp Stable Area (Medium m_z)

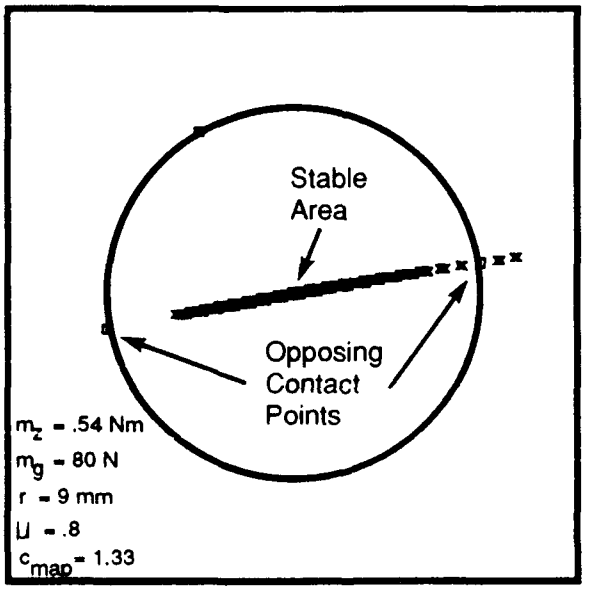

Figure 4.22. Opposing Grasp Stable Area (High m_z)

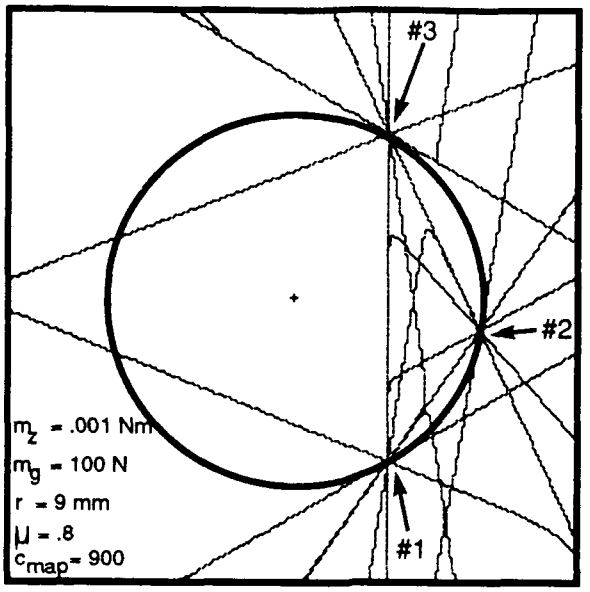

Figure 4.23. Non-enveloping Grasp Constraint Map

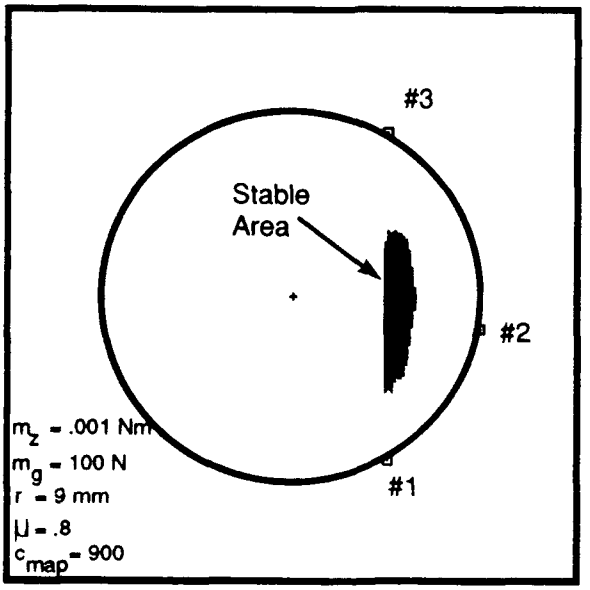

Figure 4.24. Non-enveloping Grasp Stable Area (Low m_z)

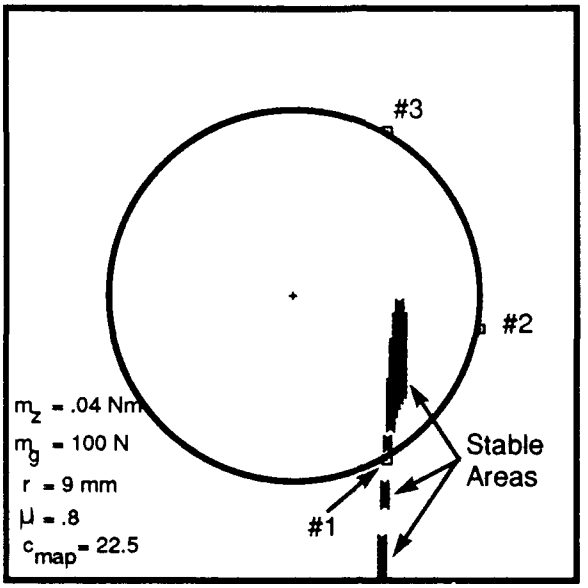

Figure 4.25. Non-enveloping Grasp Stable Area (Medium m_z)

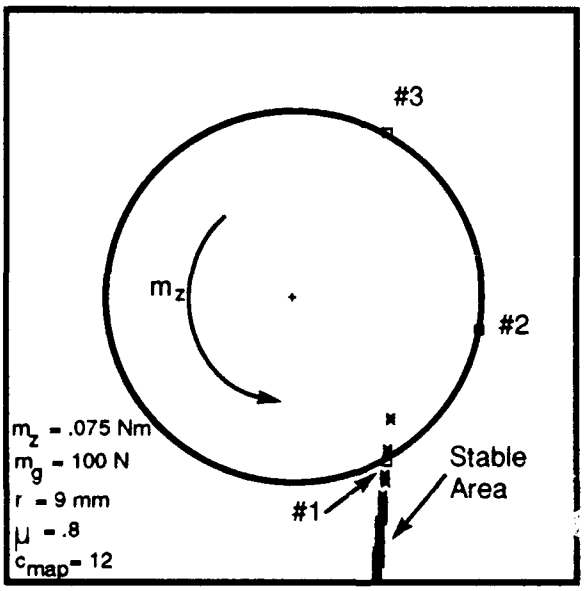

Figure 4.26. Non-enveloping Grasp Stable Area (High m_z)

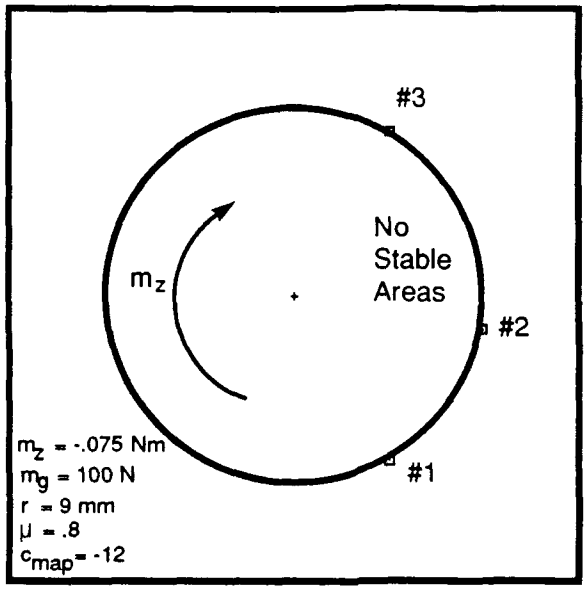

Figure 4.27. Negative Torque, No Stable Area

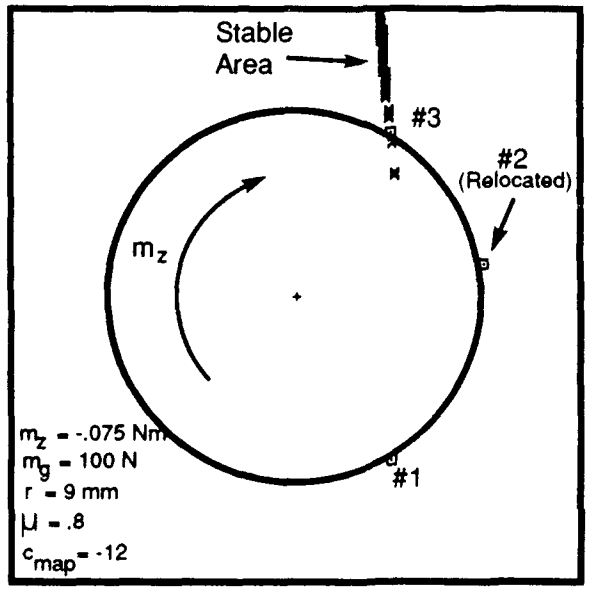

Figure 4.28. Negative Torque, Stable Area Returns

changes from an oval area near the center of the contact triangle to a thin line just outside the leading contact point. Investigation has shown that the enveloping and opposing grasps are relatively unaffected by torque direction.

4.3 The Power Grasp

In the case of the single finger power grasp we have one finger trying to achieve a stable grasp where there were three fingers with the fingertip grasp. With one finger doing the work of three, greater joint torques will need to be applied, and torque violations are more likely for similar external torque levels.

The approach in this section is to use the specific power grasp chosen in Section 3.2.3, and then map where the stable area is for a low level of external torque. At this point there will be no joint torque violations. Next, the external torque is increased in increments, but the c_{map} value is kept constant by also increasing m_g. Since the c_{map} value is constant, the size and shape of the stable area will remain constant. However, as m_z is increased an "unsafe" area will appear and grow larger. This is an area where joint torque limits are exceeded, and it must be avoided. Ultimately, the choice for grasp force focus location will be limited to areas that are both safe *and* stable.

4.3.1 Initial Stable Area. The chosen grasp configuration for the 9 mm radius cylinder has the first link of the finger contacting at 270° with the finger wrapped over the "top" of the cylinder. The second and third contact points were measured as being at 355°, and 80°, respectively. This puts the grasp in the non-enveloping category, and notice that there is an 85° separation between both the first and second contacts and the second and third contacts. The value of m_z is initially set at .03 Nm, and m_g is set at 16.67 Nm. A 9 mm cylinder radius puts the value of c_{map} at 5. The friction coefficient will be kept at .8. Figure 4.29 shows the constraint map, and Figure 4.30 shows the area containing the safe and stable points which are stored in the output file "SAS##.DAT" (see section III). "Safe and stable" indicates that there are no joint torque violations, and the contact code is 111.

4.3.2 Encroaching Unsafe Area. For the first increment, m_z is increased to .09 Nm, and m_y is increased to 50 N to keep the c_{map} value at 5. Figure 4.31 shows that there are now some areas where joint three torque limits are exceeded. A comparison of Figures 4.30 and 4.32 shows that these torque violations have started to reduce the size of the safe and stable area.

For increment #2, m_z is increased to .14 Nm and m_y is increased to 77.78 N, keeping c_{map} at 5. This causes the joint three torque violation area to grow larger (Figure 4.33), which further reduces the size of the safe and stable area (Figure 4.34).

The final increment uses values of .18 Nm and 100 N for m_z and m_y, respectively. At this point the safe and stable area has been reduced to a very small area just inside the first link's contact point, as shown in Figure 4.35.

4.3.3 Torque Direction Considerations. In section 4.2.3 it was demonstrated that for three-finger non-enveloping grasps the torque resistance capability is independent of torque direction if the intermediate contact point is equally separated from the leading and trailing contact points. Is this the case for single-finger power grasps? This particular grasp has equal 85° separations between adjacent contact points, implying that the torque direction shouldn't make a difference.

The external torque in Figure 4.35 is .18 Nm. If the capabilities of the grasp are torque direction independent, then there should still be safe and stable areas if $-.18\,Nm$ is used. This is not the case, however. Using a c_{map} value of -5, safe and stable areas do not reappear until the negative external torque is reduced to $-.16\,Nm$, as shown in Figure 4.36.

Therefore, due to manipulator joint torque limits, the resistance capability against positive torques is greater than that against negative torques (11 % greater using c_{map} values of 5 vs. -5). The generalization that can be made is that torque resistance capability will be greater if the distal link is used to make the trailing contact with the cylinder, and the proximal link is used for the leading contact. Note that a manipulator with different joint torque limits may not comply with this generalization.

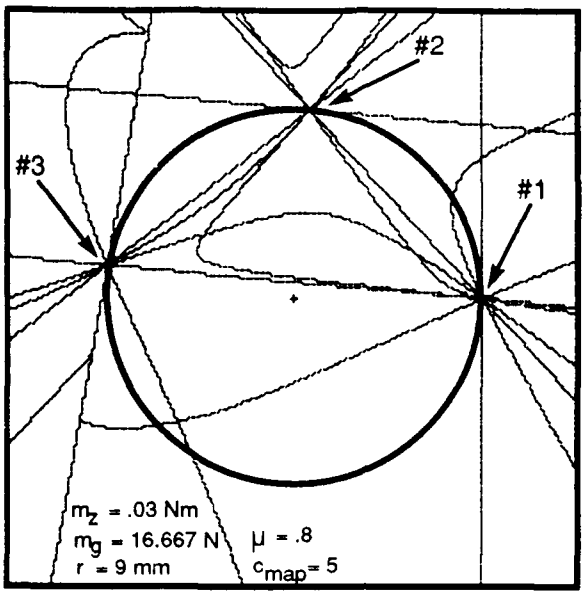

Figure 4.29. Power Grasp Constraint Map

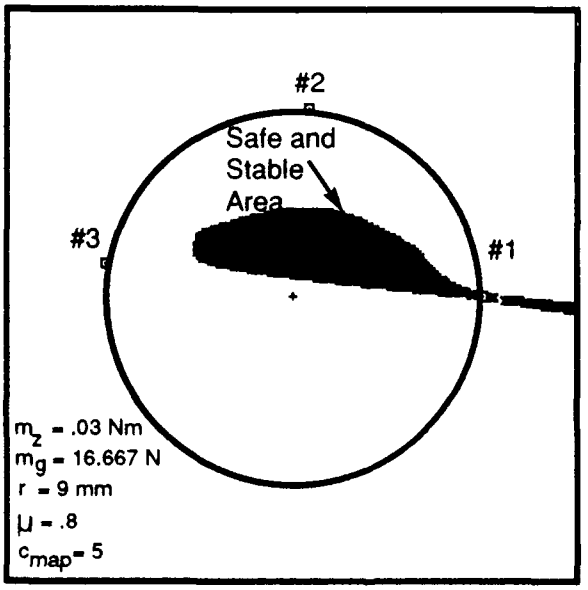

Figure 4.30. Safe and Stable Area ("Start")

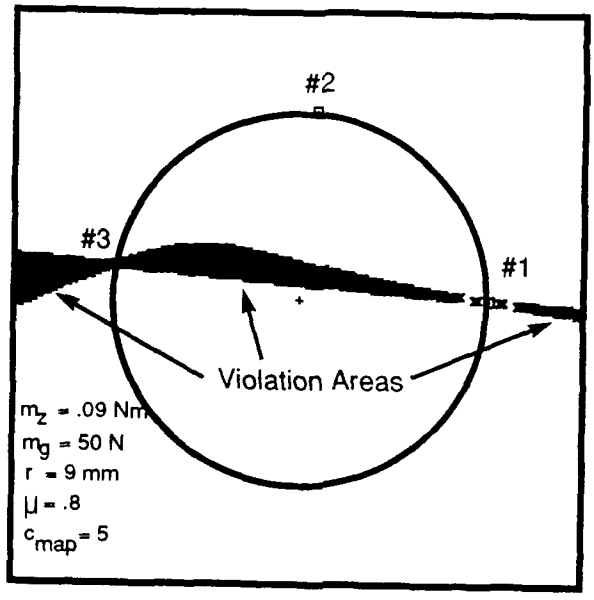

Figure 4.31. Joint 3 Torque Violations (Incr. #1)

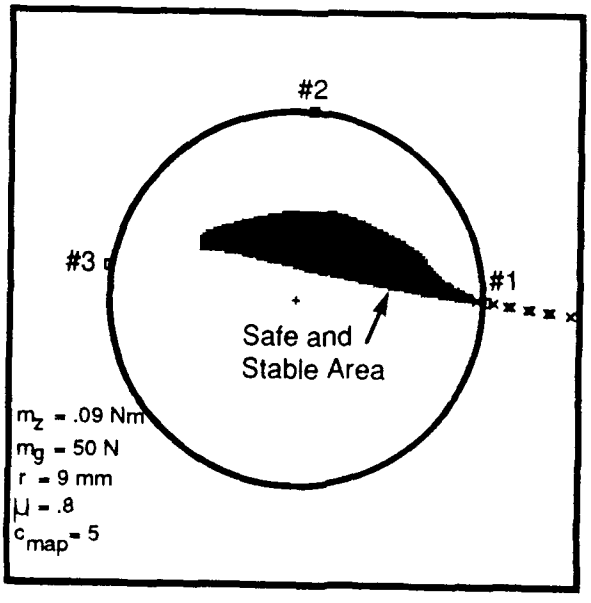

Figure 4.32. Safe and Stable Area (Incr. #1)

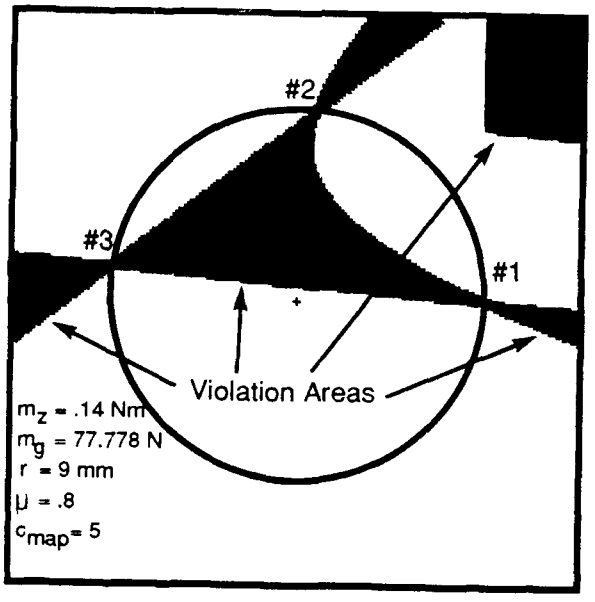

Figure 4.33. Joint 3 Torque Violations (Incr. #2)

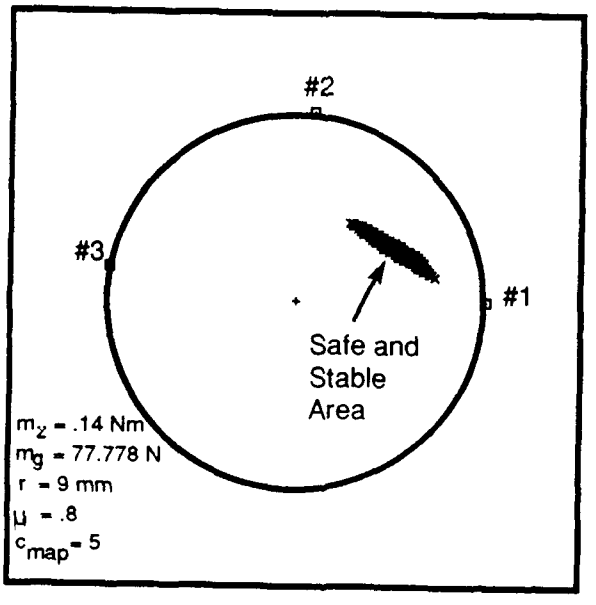

Figure 4.34. Safe and Stable Area (Incr. #2)

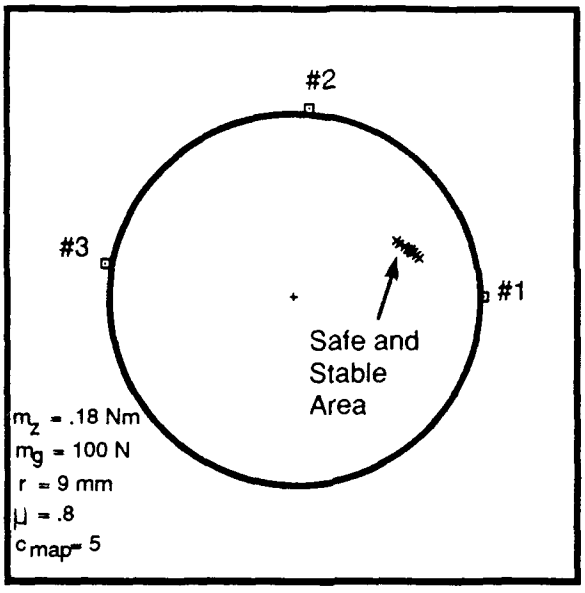

Figure 4.35. Safe and Stable Area (Incr. #3)

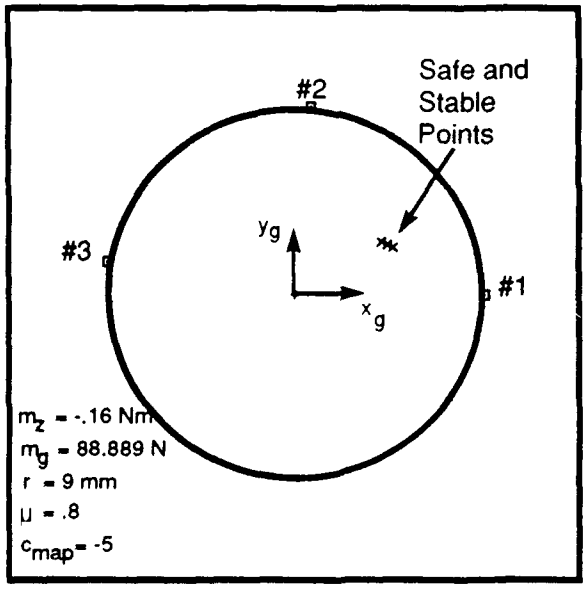

Figure 4.36. Maximum Negative Torque Resistance

The joint torque limits for a UMDH finger are roughly proportional to those of a human finger. Therefore, it should be possible to substantiate this conclusion by examining how humans prefer to grasp a cylindrical object that they intend to exert torques upon. For an object roughly the size of an oil filter a human will position his grasp so that the fingers wrap around one direction, and the thumb the other. The torque direction that is preferred is the one that makes the fingertip contacts the trailing contacts. Since the fingertips are the most distal links of human fingers, the human preference matches that of the grasp examined here.

4.3.4 Use of Minumum c_{map} Value. To this point all of the maps for the power grasp have used a c_{map} value of 5 (or -5). Using a c_{map} value of 5, the capabilities of the manipulator are about to be exceeded for an external moment of $.18\,Nm$. Will using a smaller c_{map} value produce better results? Investigation reveals that for this specific grasp the strictly stable area (torque limits are not yet considered) has almost disappeared for a c_{map} value of 1.68, as indicated in Figure 4.37. This value of 1.68 is used as the "minimum c_{map} value" for this specific case. Keeping this value constant, unsafe areas will start to appear as m_z is again increased. If the unsafe area moves over the small remaining stable area, then the capabilities of the manipulator have been exceeded since no safe and stable areas remain.

Figure 4.38 shows that for an m_z value of $.25\,Nm$ the encroaching unsafe area has caused the safe and stable area to be reduced to a single point. This value of external torque is the largest amount that can be resisted by this manipulator using this grasp geometry. This torque can only be resisted if the focus is located at the safe and stable point indicated in Figure 4.38. This focus location corresponds to the best possible contact force solution for resisting external torques.

4.4 Summary

Investigation of three-finger grasp constraint maps revealed that independent increases in m_g, r, and μ all cause the size of the stable area to increase. An independent increase in m_z invariably caused the size of the stable area to decrease. Examination of

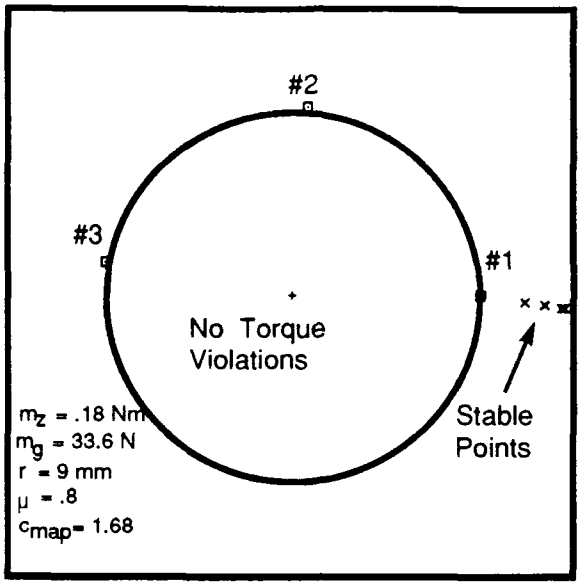

Figure 4.37. Minimum c_{map} Stable Area

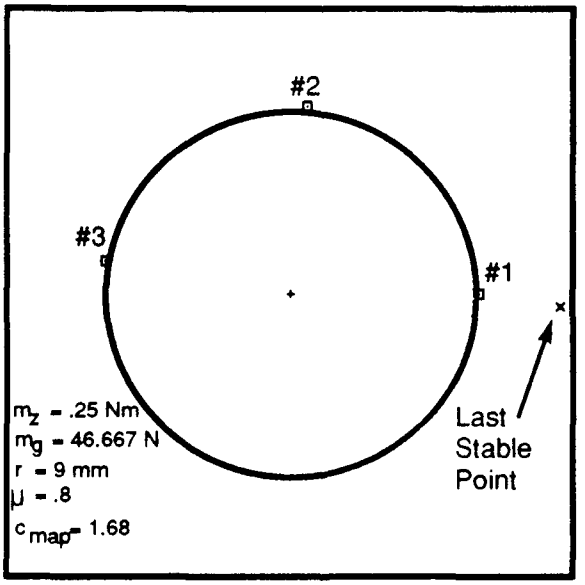

Figure 4.38. Maximum Torque Resistance

the constraint equations showed that, for a specific grasp geometry and friction coefficient, the constraint map remains unchanged if c_{map} is kept constant ($c_{map} \equiv \frac{m_y r}{m_z}$).

The three categories of grasp geometries (enveloping, opposing, and non-enveloping) each have unique properties with regard to stable area locations and minimum c_{map} values (the value of c_{map} at stable area disappearance). For enveloping grasps the stable area always disappears at the center of the cylinder. For opposing grasps the stable area reduces to a line between the two opposing contact points. For non-enveloping grasps the stable area reduces to a short line, just outside the leading contact point, which must be determined graphically. Greater envelopment of the object allows c_{map} to go to a smaller value before the stable area disappears, implying greater grasp "efficiency". The non-enveloping grasp is the only category which demonstrated a significant direction dependence with respect to torque resistance capability.

The method was successfully applied to a specific single-finger power grasp. The results show that, for the UMDH finger, greater torque resistance is possible if the distal link is used as the trailing contact. For maximum torque resistance capability the minimum c_{map} value should be used, and the grasp force focus located at the last remaining stable point. Keeping c_{map} constant as the external torque is increased ensures that the constraint map does not change, and that the grasp force focus stays in the stable area. This results in the greatest possible torque resistance capability for the grasp.

V. Conclusions

Most of the conclusions drawn from the results of this study are manipulator dependent as well as grasp dependent, and given the graphical nature of the results it is difficult to give exact answers to the question, "which contact solution is best". However, the method presented here for constraint map generation and focus placement can be applied to any three-point grasp of a cylindrical object, as well as any specific manipulator. In every case the "best" grasp force focus location can be determined graphically by using a map which shows which grasp force focus locations will result in stable grasps that do not violate the capabilities of the manipulator. The coordinates for the focus point and the value of m_g can be used to solve for the contact forces, and thus for the required joint torques or tendon tensions. This will ensure the greatest possible torque resistance capability for the manipulator.

Examination of fingertip grasps, where manipulator capabilities are disregarded, yielded valuable insight into how the stable area of the constraint map responded to changes in variables such as: external torque (m_z), grasp force magnitude (m_g), cylinder radius (r), friction coefficient, and contact locations. Theoretical analysis and demonstration revealed that if the value of c_{map} (defined as $\frac{m_g r}{m_z}$) is kept constant, then the constraint map will remain unchanged, given a fixed grasp geometry and friction coefficient. This property can be exploited for purposes of method implementation. While grasping a cylindrical object of fixed radius, the level of m_g can be scaled to the measured m_z value in order to keep c_{map} constant. Thus, movement of the stable area is prevented, allowing the grasp force focus to be located at one point continually.

The exact point at which the grasp force focus should be placed is grasp dependent. Three categories of grasp geometry were defined and examined. For enveloping grasps, where the maximum angular separation between two adjacent contact points is less than 180°, the stable area always shrinks to a point at the center of the cylinder as the external torque is (independently) increased. For opposing grasps, where two contact points are exactly 180° apart, the stable area reduces to a line between the two opposing contact points. For non-enveloping grasps, where the maximum angular separation between two

adjacent contact points is greater than 180°, the point at which the stable area disappears must be determined graphically.

This stable area disappearance point is important since locating the grasp force focus at that point allows the value of c_{map} to shrink to the smallest possible value before the grasp begins to slip. This "minimum c_{map} value" implies maximum grasp efficiency (the greatest amount of external torque that can be resisted for a given grasp force magnitude). Of the three grasp geometries, the minimum c_{map} was lowest for the enveloping grasp, and highest for the non-enveloping grasp. This trend indicates that greater invelopment is desireable since it gives the grasp greater efficiency.

The non-enveloping grasp geometry has unique properties. The three contact points are clustered on one side of the cylinder. If a circular arrow is drawn, indicating the direction of the external torque, then the first contact point the arrow reaches in the cluster is designated the "leading contact point". The next point is the "intermediate contact point", and finally there is the "trailing contact point". It was observed that if the intermediate contact point is located mid-way between the leading and trailing contact points, then the torque resistance capability of the grasp will be direction independent. If the intermediate contact point is located closer to one of the other two points, then the torque resistance capability will be greater if the torque direction is chosen such that the point in closer proximity to the intermediate point is the leading contact point. The other two grasp types did not exhibit any obvious "preference" for torque direction.

Another unique property of non-enveloping grasps is that the stable area changes location as the external torque is independently increased. The stable area starts as an oval near the center of the triangle formed by the three contact points, and then moves toward the leading contact point as it shrinks. Just before disappearance the stable area has been reduced to a short line just outside the leading contact point. This stable area movement can be prevented if c_{map} is kept constant, as previosly discussed. This allows the grasp force focus to be placed at a single point which remains "stable" as the external torque is increased.

The main objective of this study was to apply the grasp force focus placement method

to a specific, three-point contact, single-finger power grasp using a finger of the Utah/MIT Dextrous Hand as the manipulator. This objective was successfully accomplished. The limitations of the manipulator were modeled as joint torque violation areas on the constraint map, where it would be "unsafe" to locate the grasp force focus. The behavior of the unsafe areas revealed an almost "human" torque direction preference for the UMDH finger. The torque resistance capability was found to be greater if the torque direction was chosen such that the distal link was made to be the trailing contact point. Humans tend to have the same preference for torque direction when exerting torques on cylindrical objects.

The maximum torque resistance capabilities of the grasp and manipulator were realized by employing the minimum c_{map} value and locating the grasp force focus at the last remaining stable point. Keeping c_{map} constant, the external torque could be increased to $.25\,Nm$ before the last stable point was covered by the unsafe area, thus exceeding the capabilities of the manipulator.

VI. Recommendations

6.1 More than Three Contact Points

This study was initiated as a first step in solving one portion of an intelligent part mating problem; fitting an oil filter onto a threaded post using a dextrous robotic manipulator. The final stage of the problem is to use a power grasp to tighten the filter onto the base of the post. This project examined a simplified three-point power grasp, thus my first recommendation concerns the matter of extending the scope of this project to include more complicated grasps.

The method of grasp force focus placement is currently limited to three-point grasps due to the fact that a focus isn't guaranteed to exist for a grasp that has more than three contact points. However, it should be possible to constrain the internal contact forces to produce a focus point even for grasps of four or more contacts. In fact, the contact points need not even be coplanar. This would require three-dimensional mapping, but it is theoretically possible.

If such a study was made it would be prudent to determine whether or not the benefits gained from focus placement methods outweigh any limitations placed on the manipulator from contact force constraints. It is reasonable to assume that this method could eventually be applied to multifinger grasps with multiple contacts per finger. Such a grasp would be ideal for the final stage of the chosen part mating task.

6.2 Real-Time Implementation

The results of this study would be put to greatest use by implementing the methods described herein as a real-time algorithm. The most calculation-intensive aspect of the method involves the determination of the minimum c_{map} value and the coordinates of the last remaining stable point. These calculations could be accomplished as part of the grasp planning phase. Keeping the c_{map} value constant would require accurate sensor data for the external torque being applied to the object. This would allow proper scaling of the grasp force magnitude, thus preventing movement of the stable area.

6.3 Staying with Three-Point Grasps

This study has shown that the focus placement method can be used to maximize torque resistance capabilities for a three-point grasp. However, there is no reason this method could not be used for other manipulation tasks using three-point grasps which involve a combination of external forces and moments on the grasped object. The benefit of staying with three-point grasps is that the constraints on the internal contact forces are much simpler, and a two-dimensional constraint map is always sufficient.

6.4 Manipulator Optimization

All of the torque violation areas mapped in Chapter IV were due to joint 3 violations. The torque resistance capabilities of the chosen manipulator could be greatly enhanced by increasing the tension capabilities of the joint 3 flexor tendon. Further enhancement could be realized if the tendon tension capabilities were optimized to allow the greatest possible torque resistance. This optimization would be task specific, but the potential for improvement does exist.

6.5 Friction

The ability to increase static friction between the object and the manipulator was not examined in this study. High friction coatings, etc. could greatly increase the torque resistance capability of a grasp. Also, realistic results from the focus placement method can only be expected if realistic friction coefficients are used. A more accurate friction *model* could also help improve the accuracy of these results.

Appendix A. *Internal Contact Force Solution*

Internal Contact Force Solution

- Goal: solve for... $\bar{c}_h = (x_1,\ z_1,\ x_2,\ z_2,\ x_3,\ z_3)^t$
- Need 6 *linearly independent* constraint equations;
  1. Equation 2.8 ... 1 constraint
  2. Equations 2.10 ... 3 constraints
  3. $\sum F_x = 0 \quad \sum F_y = 0 \quad \sum M_z = 0 \ldots 3$ constraints
- The six equations represented by items 2) and 3) can be arranged in matrix form;

Row #

$$
\begin{array}{c}
(1) \\ (2) \\ (3) \\ (4) \\ (5) \\ (6)
\end{array}
\left[\begin{array}{cc}
x_g sin\phi_1 - y_g cos\phi_1 + r & x_g cos\phi_1 + y_g sin\phi_1 \\
0 & 0 \\
0 & 0 \\
-cos\phi_1 & sin\phi_1 \\
sin\phi_1 & cos\phi_1 \\
1 & 0
\end{array}\right.
$$

$$
\left.\begin{array}{cc}
0 & 0 \\
x_g sin\phi_2 - y_g sin\phi_2 + r & x_g cos\phi_2 + y_g sin\phi_2 \\
0 & 0 \\
-cos\phi_2 & sin\phi_2 \\
sin\phi_2 & cos\phi_2 \\
1 & 0
\end{array}\right.
$$

$$
\left.\begin{array}{cc}
0 & 0 \\
0 & 0 \\
x_g sin\phi_3 - y_g cos\phi_3 + r & x_g cos\phi_3 + y_g sin\phi_3 \\
-cos\phi_3 & sin\phi_3 \\
sin\phi_3 & cos\phi_3 \\
1 & 0
\end{array}\right]
\left(\begin{array}{c} x_1 \\ z_1 \\ x_2 \\ z_2 \\ x_3 \\ z_3 \end{array}\right)
=
\left(\begin{array}{c} 0 \\ 0 \\ 0 \\ 0 \\ 0 \\ 0 \end{array}\right)
$$

- Gaussian elimination can be applied to the above coefficient matrix
- Linear dependence is eliminated by replacing row (6) (New rows are designated by ( )*);

$$
\begin{aligned}
(6)^* &= (1) + (2) + (3) - y_g(4) - x_g(5) - r(6) \\
&= (0 \quad 0 \quad 0 \quad 0 \quad 0 \quad 0) \leftarrow \textit{all coefficients zero}
\end{aligned}
$$

- Rearranging rows and rewriting the coefficient matrix;

$$
\begin{bmatrix}
1 & 0 & 1 & 0 & 1 & 0 \\
-cos\phi_1 & sin\phi_1 & -cos\phi_2 & sin\phi_2 & -cos\phi_3 & sin\phi_3 \\
sin\phi_1 & cos\phi_1 & sin\phi_2 & cos\phi_2 & sin\phi_3 & cos\phi_3 \\
0 & 0 & x_g sin\phi_2 - y_g cos\phi_2 + r & x_g cos\phi_2 + y_g sin\phi_2 & 0 & 0 \\
0 & 0 & 0 & 0 & x_g sin\phi_3 - y_g cos\phi_3 + r & x_g cos\phi_3 + y_g sin\phi_3 \\
0 & 0 & 0 & 0 & 0 & 0
\end{bmatrix}
$$

- Replace elements with the following parameters;

$$
\begin{aligned}
P_1 &= -cos\phi_1 & P_7 &= x_g sin\phi 2 - y_g cos\phi 2 + r \\
P_2 &= sin\phi_1 & P_8 &= x_g cos\phi 2 + y_g sin\phi 2 \\
P_3 &= -cos\phi_2 & P_9 &= x_g sin\phi 3 - y_g cos\phi 3 + r \\
P_4 &= sin\phi_2 & P_{10} &= x_g cos\phi 3 + y_g sin\phi 3 \\
P_5 &= -cos\phi_3 & & \\
P_6 &= sin\phi_3 & &
\end{aligned}
$$

- Rewrite matrix;

$$\begin{array}{c} (1) \\ (2) \\ (3) \\ (4) \\ (5) \\ (6) \end{array} \begin{bmatrix} 1 & 0 & 1 & 0 & 1 & 0 \\ P_1 & P_2 & P_3 & P_4 & P_5 & P_6 \\ P_2 & -P_1 & P_4 & -P_3 & P_6 & -P_5 \\ 0 & 0 & P_7 & P_8 & 0 & 0 \\ 0 & 0 & 0 & 0 & P_9 & P_{10} \\ 0 & 0 & 0 & 0 & 0 & 0 \end{bmatrix}$$

- Eliminate first element in rows (2) and (3);

$$(2)' = (2) - P_1(1)$$
$$(3)' = (3) - P_2(1)$$

- Eliminate second element in row (3);

$$(3)'' = (3)' - \frac{P_4}{P_7}(2)$$

- Rewrite using substituted parameters;

$$\begin{array}{c} (1) \\ (2) \\ (3) \\ (4) \\ (5) \\ (6) \end{array} \begin{bmatrix} 1 & 0 & 1 & 0 & 1 & 0 \\ 0 & P_2 & Q_1 & P_4 & Q_2 & P_6 \\ 0 & 0 & Q_3 & Q_4 & Q_5 & Q_6 \\ 0 & 0 & P_7 & P_8 & 0 & 0 \\ 0 & 0 & 0 & 0 & P_9 & P_{10} \\ 0 & 0 & 0 & 0 & 0 & 0 \end{bmatrix}$$

where;

$$
\begin{aligned}
Q_1 &= P_3 - P_1 \\
Q_2 &= P_5 - P_1 \\
Q_3 &= P_1P_2 + P_1P_3 - P_2^2 - P_1^2 \\
Q_4 &= P_4P_1 - P_3P_2 \\
Q_5 &= P_6P_2 + P_1P_5 - P_2^2 - P_1^2 \\
Q_6 &= P_1P_6 - P_5P_2
\end{aligned}
$$

- Continue eliminating elements both above and below the main diagonal;

$$
\begin{aligned}
(1)^* &= \left[(1) - \tfrac{1}{Q_3}(3)\right] Q_3 \\
(2)^* &= \left[(2) - \tfrac{Q_4}{Q_3}(3)\right] Q_3 \\
(4)^* &= \left[(4) - \tfrac{P_7}{Q_3}(3)\right] Q_3
\end{aligned}
$$

gives;

$$
\begin{bmatrix}
Q_3 & 0 & 0 & -Q_4 & Q_3 - Q_5 & -Q_6 \\
0 & Q_3P_2 & 0 & R_1 & R_2 & R_3 \\
0 & 0 & Q_3 & Q_4 & Q_5 & Q_6 \\
0 & 0 & 0 & R_4 & R_5 & R_6 \\
0 & 0 & 0 & 0 & P_9 & P_{10} \\
0 & 0 & 0 & 0 & 0 & 0
\end{bmatrix}
$$

where;

$$R_1 = P_1Q_3 - Q_1Q_4$$
$$R_2 = Q_2Q_3 - Q_1Q_5$$
$$R_3 = P_6Q_3 - Q_1Q_6$$
$$R_4 = P_8Q_3 - P_7Q_4$$
$$R_5 = -Q_5P_7$$
$$R_6 = -Q_6P_7$$

- Continue in this manner until the matrix is reduced to;

$$\begin{bmatrix} P_9Q_3R_1 & 0 & 0 & 0 & 0 & V_1 \\ 0 & P_2P_9Q_3R_1 & 0 & 0 & 0 & V_2 \\ 0 & 0 & P_9Q_3R_1 & 0 & 0 & V_3 \\ 0 & 0 & 0 & P_9R_1 & 0 & V_4 \\ 0 & 0 & 0 & 0 & P_9 & P_{10} \\ 0 & 0 & 0 & 0 & 0 & 0 \end{bmatrix} \equiv [A]$$

where;

$$U_1 = Q_3R_4 - Q_5R_4 + Q_4R_5$$
$$U_2 = Q_4R_6 - Q_6R_4$$
$$U_3 = R_2R_4 - R_1R_5$$
$$U_4 = R_3R_4 - R_1R_6$$
$$U_5 = Q_5R_4 - Q_4R_5$$
$$U_6 = Q_6R_4 - Q_4R_6$$

and;

$$V_1 = U_2P_9 - U_4P_{10}$$
$$V_2 = U_4P_9 - U_3P_{10}$$
$$V_3 = U_6P_9 - U_5P_{10}$$
$$V_4 = R_6P_9 - R_5P_{10}$$

- Since $[A]\,\bar{c}_h = \bar{0}$;

$$x_{1_i} = W_1 z_{3_i}$$
$$z_{1_i} = W_2 z_{3_i}$$
$$x_{2_i} = W_3 z_{3_i}$$
$$z_{2_i} = W_4 z_{3_i}$$
$$x_{3_i} = W_5 z_{3_i}$$

where;

$$W_1 = \frac{V_1}{P_3 Q_3 R_3}$$
$$W_2 = \frac{V_2}{P_2 P_3 Q_3 R_3}$$
$$W_3 = \frac{V_3}{P_3 Q_3 R_3}$$
$$W_4 = \frac{V_4}{P_3 R_3}$$
$$W_5 = \frac{-P_{3_0}}{P_3}$$

- Equation 2.8 can now be used to solve for z_{3_i} (given m_g);

$$m_g = \sqrt{x_{1_i}^2 + z_{1_i}^2} + \sqrt{x_{2_i}^2 + z_{2_i}^2} + \sqrt{x_{3_i}^2 + z_{3_i}^2}$$

therefore;

$$z_{3_i} = \frac{m_g}{\sqrt{W_1^2 + W_2^2} + \sqrt{W_3^2 + W_4^2} + \sqrt{W_5^2 + 1}}$$

- Back substitution is used to solve for the other elements of $\bar{c}_h$.

Appendix B. *Computer Listing*

```
      PROGRAM MAPPER

CCCCCCCCCCCCCCCCCCCCCCCCCCCCCCCCCCCCCCCCCCCCCCCCCCCCCCCCCCCCCCCCCCCC
CC  THIS IS MAPPER.  IT IS A FORTRAN PROGRAM THAT GENERATES     CC
CC  DATA FOR CONSTRAINT MAPS.  NO SUBROUTINES ARE CALLED, IT    CC
CC  JUST RUNS STRAIGHT THROUGH...IT IS EXPLAINED WELL WITH      CC
CC  COMMENTS THOUGH, SO I DON'T WANT TO HEAR ANY COMPLAINTS     CC
CC  ABOUT NOT BEING ABLE TO DECIPHER MY CODE.                   CC
CC      INPUTS:                                                 CC
CC         PHI1,PHI2,PHI3.......CONTACT POINT LOCATIONS FROM    CC
CC                              VERTICAL, GOING CNTR-CLKWSE     CC
CC         MZ...................EXTERNAL MOMENT APPLIED         CC
CC         MG...................GRASP FORCE MAGNITUDE           CC
CC         R....................CYLINDER RADIUS                 CC
CC         MU...................FRICTION COEFFICIENT (STATIC)   CC
CC         S....................SCALE OF MAP (THE NUMBER OF     CC
CC                              CYLINDER RADII FROM THE CENTER  CC
CC                              TO THE EDGE OF THE MAP)         CC
CC         RUN..................A TWO DIGIT CHARACTER STRING    CC
CC                              USED TO I.D. GENERATED FILES    CC
CC         RESX,RESY............MAP RESOLUTION (HORIZ & VERT)   CC
CC                                                              CC
CC      INPUTS FROM HAND.DAT:                                   CC
CC         L1,L2................1st AND 2nd FINGER LENGTHS      CC
CC         A1,A2,A3.............DISTANCE FROM (i)th JOINT TO    CC
CC                              (i)th CONTACT POINT (i=1,2,3)   CC
CC         THETA1,2,3...........D&H LINK POSITION ANGLES        CC
CC         THI,II,III...........THETA1,2,3 PLUS ANGLE DOWN TO   CC
CC                              LINE JOINING JOINT & CONTACT PT CC
CC         TAU1,2,3MX...........JOINT TORQUE LIMITS            CC
CC         GAMMA................OFFSET ANGLE OF THIRD CONTACT   CC
CC                              TANGENTIAL DIRECTION WITH       CC
CC                              RESPECT TO LINK 3 MID-LINE      CC
CC                                                              CC
CC      OUTPUT FILES:           (## = RUN NUMBER)               CC
CC         STABLE##.DAT.........DATA POINTS INDICATING AREAS    CC
CC                              WITH A STABLE CODE (111)        CC
CC         BNDRY##.DAT..........DATA POINTS FOR BOUNDARIES      CC
CC                              BETWEEN DIFFERENT CODE AREAS    CC
CC         CNTCTS##.DAT.........DATA POINTS FOR LOCATIONS OF    CC
CC                              CONTACT POINTS                  CC
CC         JTONE##.DAT..........POINTS WHERE JOINT ONE TORQUE   CC
CC                              LIMITS ARE EXCEEDED             CC
CC         JTTWO##.DAT..........POINTS WHERE JOINT TWO TORQUE   CC
CC                              LIMITS ARE EXCEEDED             CC
CC         JTTHR##.DAT..........POINTS WHERE JOINT THREE TORQUE CC
CC                              LIMITS ARE EXCEEDED             CC
CC         SAS##.DAT............SAFE AND STABLE AREAS           CC
CC                                                              CC
CCCCCCCCCCCCCCCCCCCCCCCCCCCCCCCCCCCCCCCCCCCCCCCCCCCCCCCCCCCCCCCCCCCC

      INTEGER CODE,CODE1,CODE2,CODE3,CODEPR,END
      REAL MU,MG,MZ,L1,L2
      CHARACTER RUN*2,ANS*1,YES*1,SYES*1

      TYPE *,'*******************************************************'
```

```
      TYPE *,'********************************************************'
      TYPE *,'**                                                    **'
      TYPE *,'**  *      *     **     ****   ****   ******  ****    **'
      TYPE *,'**  **    **    *  *    *   *  *   *  *       *   *   **'
      TYPE *,'**  * *  * *   *    *   *   *  *   *  *       *   *   **'
      TYPE *,'**  *  **  *   ******   ****   ****   ****    ****    **'
      TYPE *,'**  *      *  *      *  *      *      *       *  *    **'
      TYPE *,'**  *      *  *      *  *      *      *       *   *   **'
      TYPE *,'**  *      *  *      *  *      *      ******  *    *  **'
      TYPE *,'**                                                    **'
      TYPE *,'********************************************************'
      TYPE *,'********************************************************'
      TYPE *,' '
      TYPE *,' '
      TYPE *,' '
      TYPE *,' '
      TYPE *,' '
      TYPE *,' '
      TYPE *,' '
      TYPE *,' '

CCCCCCCCCCCCCCCCCCCCCCCCCCCCCCCCC
C                               C
C   PROMPT FOR VARIOUS INPUTS   C
C                               C
CCCCCCCCCCCCCCCCCCCCCCCCCCCCCCCCC

      TYPE *,'INPUT PHI1, PHI2, PHI3 (Deg);'
      ACCEPT *, PHI1,PHI2,PHI3
      TYPE *,'INPUT MOMENT APPLIED (N-m);'
      ACCEPT *, MZ
      TYPE *,'INPUT GRASP FORCE MAGNITUDE (N);'
      ACCEPT *, MG
      TYPE *,'INPUT CYLINDER RADIUS (m);'
      ACCEPT *, R
      TYPE *,'INPUT FRICTION COEFFICIENT;'
      ACCEPT *, MU
      TYPE *,'MAP SCALE ?'
      ACCEPT *, S
      TYPE *,'RUN NUMBER ? (2-DIGIT)'
      READ(5,10)RUN
 10   FORMAT(A)
      TYPE *,'X-RESOLUTION,Y-RESOLUTION (EVEN NUMBERS);'
      ACCEPT *, RESX,RESY
      TYPE *,'DO YOU WANT EXTRA BOUNDARY RESOLUTION (Y/N)?'
      READ(5,20)ANS
 20   FORMAT(A)
      YES='Y'
      SYES='y'

CCCCCCCCCCCCCCCCCCCCCCCCCCCCCCCCCCCCCCCCCCCCCCCCCC
C                                                C
C   USE OPEN STATEMENTS TO ASSOCIATE FILENAMES    C
C        WITH VARIOUS LOGICAL UNIT NUMBERS       C
C                                                C
CCCCCCCCCCCCCCCCCCCCCCCCCCCCCCCCCCCCCCCCCCCCCCCCCC
```

```
107         OPEN(12,FILE='HAND.DAT',STATUS='OLD',
108        1        ACCESS='SEQUENTIAL',
109        1        FORM='FORMATTED')

110         OPEN(13,FILE='JTONE'//RUN//'.DAT',STATUS='NEW',
111        1        ACCESS='SEQUENTIAL',
112        1        FORM='FORMATTED')

113         OPEN(14,FILE='JTTWO'//RUN//'.DAT',STATUS='NEW',
114        1        ACCESS='SEQUENTIAL',
115        1        FORM='FORMATTED')

116         OPEN(15,FILE='JTTHR'//RUN//'.DAT',STATUS='NEW',
117        1        ACCESS='SEQUENTIAL',
118        1        FORM='FORMATTED')

119         OPEN(16,FILE='STABLE'//RUN//'.DAT',STATUS='NEW',
120        1        ACCESS='SEQUENTIAL',
121        1        FORM='FORMATTED')

122         OPEN(17,FILE='BNDRY'//RUN//'.DAT',STATUS='NEW',
123        1        ACCESS='SEQUENTIAL',
124        1        FORM='FORMATTED')

125         OPEN(18,FILE='CNTCTS'//RUN//'.DAT',STATUS='NEW',
126        1        ACCESS='SEQUENTIAL',
127        1        FORM='FORMATTED')

128         OPEN(19,FILE='SAS'//RUN//'.DAT',STATUS='NEW',
129        1        ACCESS='SEQUENTIAL',
130        1        FORM='FORMATTED')

131   CCCCCCCCCCCCCCCCCCCCCCCCCCCCCCCCCCCCC
132   C                                    C
133   C   INPUT DATA FROM HAND.DAT FILE     C
134   C                                    C
135   CCCCCCCCCCCCCCCCCCCCCCCCCCCCCCCCCCCCC

136         READ(12,100)A1
137         READ(12,100)A2
138         READ(12,100)A3
139         READ(12,100)L1
140         READ(12,100)L2
141         READ(12,100)THETA1
142         READ(12,100)THETA2
143         READ(12,100)THETA3
144         READ(12,100)THI
145         READ(12,100)THII
146         READ(12,100)THIII
147         READ(12,100)TAU1MX
148         READ(12,100)TAU2MX
149         READ(12,100)TAU3MX
150         READ(12,100)GAMMA
151   100   FORMAT(F7.3)
```

```
152  CCCCCCCCCCCCCCCCCCCCCCCCCCCCCCCCCC
153  C                                  C
154  C   SET TOGGLE SWITCHES TO ZERO    C
155  C                                  C
156  CCCCCCCCCCCCCCCCCCCCCCCCCCCCCCCCCC

157         TOGL1=0
158         TOGL2=0
159         TOGL3=0
160         TOGL11=0

161  CCCCCCCCCCCCCCCCCCCCCCCCCC
162  C                         C
163  C   CONVERT TO RADIANS    C
164  C                         C
165  CCCCCCCCCCCCCCCCCCCCCCCCCC

166         PHI1=PHI1*3.1415926/180.0
167         PHI2=PHI2*3.1415926/180.0
168         PHI3=PHI3*3.1415926/180.0
169         THETA1=THETA1*3.1415926/180.0
170         THETA2=THETA2*3.1415926/180.0
171         THETA3=THETA3*3.1415926/180.0
172         THI=THI*3.1415926/180.0
173         THII=THII*3.1415926/180.0
174         THIII=THIII*3.1415926/180.0
175         GAMMA=GAMMA*3.1415926/180.0

176  CCCCCCCCCCCCCCCCCCCCCCCCCCCCCCCCCCCCCCCCCCCCCCCCCC
177  C                                                 C
178  C   CALCULATE 'EXTERNAL' OR BALANCING FORCES      C
179  C                                                 C
180  CCCCCCCCCCCCCCCCCCCCCCCCCCCCCCCCCCCCCCCCCCCCCCCCCC

181         B1=COS(PHI2)-COS(PHI1)
182         B2=COS(PHI2)-COS(PHI3)
183         B3=COS(PHI3)-COS(PHI1)
184         B4=SIN(PHI1-PHI3)-SIN(PHI1-PHI2)-SIN(PHI2-PHI3)
185         B5=-MZ*COS(PHI2)/R
186         B6=MZ*COS(PHI1)/R
187         B7=MZ*SIN(PHI1-PHI2)/R

188         X1E = B5/B1 - (B2*B7)/(B1*B4)
189         X2E = B6/B1 - (B3*B7)/(B1*B4)
190         X3E = B7/B4

191  CCCCCCCCCCCCCCCCCCCCCCCCCCCCCCCCCCCCCCCCCCCCCCCCCCCCCCCCCCCCCCCCCCCCCCCCCC
192  C                                                                       C
193  C   CALCULATE MATRIX NEEDED FOR JOINT TORQUE DETERMINATION              C
194  C                                                                       C
195  CCCCCCCCCCCCCCCCCCCCCCCCCCCCCCCCCCCCCCCCCCCCCCCCCCCCCCCCCCCCCCCCCCCCCCCCCC

196         D1=-A1*SIN(THI)
197         D2=A1*COS(THI)
198         D3=COS(THETA1)
199         D4=SIN(THETA1)
```

```
      D5=-A2*SIN(THETA1+THII)-L1*SIN(THETA1)
      D6= A2*COS(THETA1+THII)+L1*COS(THETA1)
      D7=-A2*SIN(THETA1+THII)
      D8= A2*COS(THETA1+THII)
      D9=COS(THETA1+THETA2)
      D10=SIN(THETA1+THETA2)
      D13=-A3*SIN(THETA1+THETA2+THIII)-L2*SIN(THETA1+THETA2)
      D14= A3*COS(THETA1+THETA2+THIII)+L2*COS(THETA1+THETA2)
      D11=D13-L1*SIN(THETA1)
      D12=D14+L1*COS(THETA1)
      D15=-A3*SIN(THETA1+THETA2+THIII)
      D16= A3*COS(THETA1+THETA2+THIII)
      D17=COS(THETA1+THETA2+THIII-GAMMA)
      D18=SIN(THETA1+THETA2+THIII-GAMMA)

      E1=D1*D3+D2*D4
      E2=D2*D3-D1*D4
      E3=D5*D9+D6*D10
      E4=D6*D9-D5*D10
      E5=D11*D17+D12*D18
      E6=D12*D17-D11*D18
      E7=D7*D9+D8*D10
      E8=D8*D9-D7*D10
      E9=D13*D17+D14*D18
      E10=D14*D17-D13*D18
      E11=D15*D17+D16*D18
      E12=D16*D17-D15*D18

CCCCCCCCCCCCCCCCCCCCCCCCCCCCCCCCCCCCCCCCCCCC
C                                          C
C   CALCULATE SOME NEEDED TRIG TERMS AND   C
C   INITIALIZE THE COMPARISON CODE TERM    C
C                                          C
CCCCCCCCCCCCCCCCCCCCCCCCCCCCCCCCCCCCCCCCCCCC

      P1=-1.0*COS(PHI1)
      P2=SIN(PHI1)
      P3=-1.0*COS(PHI2)
      P4=SIN(PHI2)
      P5=-1.0*COS(PHI3)
      P6=SIN(PHI3)

      CODEPR=0.0

CCCCCCCCCCCCCCCCCCCCCCCCCCCCCCCCCCCCCCCCCCCCCCCCCCC
C                                                 C
C   ITERATION LOOP TO CALCULATE INTERNAL FORCES,  C
C    GENERATE CONTACT CODES, CALCULATE REQUIRED   C
C               JOINT TORQUES, ETC.               C
C    (ONE ITERATION PER POINT ON GRASP PLANE)     C
C              ******START HERE******             C
C                                                 C
CCCCCCCCCCCCCCCCCCCCCCCCCCCCCCCCCCCCCCCCCCCCCCCCCCC

      TYPE *, 'BEGINNING PRIMARY LOOP'
      TYPE *, ' '
```

```
250         DO 150 V=1.0,RESY,1.0
251           J=RESY-V+1
252           WRITE(6,200)J
253           DO 140 U=1.0,RESX,1.0
254             XG=((U-1.0-RESX/2.0+0.5)*S*R)/(RESX/2.0-0.5)
255             YG=((1.0-V+RESY/2.0-0.5)*S*R)/(RESY/2.0-0.5)

256             P7=XG*SIN(PHI2)-YG*COS(PHI2)+R
257             P8=XG*COS(PHI2)+YG*SIN(PHI2)
258             P9=XG*SIN(PHI3)-YG*COS(PHI3)+R
259             P10=XG*COS(PHI3)+YG*SIN(PHI3)

260             Q1=P3-P1
261             Q2=P5-P1
262             Q3=P4*P2+P1*P3-P2**2.0-P1**2.0
263             Q4=P4*P1-P3*P2
264             Q5=P6*P2+P1*P5-P2**2.0-P1**2.0
265             Q6=P1*P6-P5*P2

266             R1=P4*Q3-Q1*Q4
267             R2=Q2*Q3-Q1*Q5
268             R3=P6*Q3-Q1*Q6
269             R4=P8*Q3-P7*Q4
270             R5=-1.0*Q5*P7
271             R6=-1.0*Q6*P7

272             U1=Q3*R4-Q5*R4+Q4*R5
273             U2=Q4*R6-Q6*R4
274             U3=R2*R4-R1*R5
275             U4=R3*R4-R1*R6
276             U5=Q5*R4-Q4*R5
277             U6=Q6*R4-Q4*R6

278             V1=U1*P10-U2*P9
279             V2=U3*P10-U4*P9
280             V3=U5*P10-U6*P9
281             V4=R5*P10-R6*P9

282             W1=V1/(P9*Q3*R4)
283             W2=V2/(P2*P9*Q3*R4)
284             W3=V3/(P9*Q3*R4)
285             W4=V4/(P9*R4)
286             W5=-1.0*P10/P9


287             Z3I=MG/(SQRT(W1**2+W2**2)+SQRT(W3**2+W4**2)+SQRT(W5**2+1.0))
288             X1I=W1*Z3I
289             Z1I=W2*Z3I
290             X2I=W3*Z3I
291             Z2I=W4*Z3I
292             X3I=W5*Z3I

293   CCCCCCCCCCCCCCCCCCCCCCCCCCCCCCCCCCCCCCCCCCCCCCC
294   C                                              C
295   C    CALCULATE TOTAL CONTACT FORCES NEEDED     C
296   C             AT EACH CONTACT POINT            C
```

```
297  C                                                    C
298  CCCCCCCCCCCCCCCCCCCCCCCCCCCCCCCCCCCCCCCCCCCCCCCCCCCC

299             X1T=X1E+X1I
300             X2T=X2E+X2I
301             X3T=X3E+X3I
302             Z1T=Z1I
303             Z2T=Z2I
304             Z3T=Z3I

305  CCCCCCCCCCCCCCCCCCCCCCCCCCCCCCCCCCCCCCCCCCCCCCCCCCCC
306  C                                                    C
307  C    TEST FOR CONSTRAINT COMPLIANCE                  C
308  C                                                    C
309  CCCCCCCCCCCCCCCCCCCCCCCCCCCCCCCCCCCCCCCCCCCCCCCCCCCC

310             UNSTAB=0.0
311             IF (Z1T .LE. 0) THEN
312                 CODE1=300
313                 UNSTAB=1.0
314               ELSE IF (ABS(X1T) .GE. (Z1T*MU)) THEN
315                     CODE1=200
316               ELSE
317                     CODE1=100
318             END IF

319             IF (Z2T .LE. 0) THEN
320                 CODE2=30
321                 UNSTAB=1.0
322               ELSE IF (ABS( . ) .GE. (Z2T*MU)) THEN
323                     CODE2=20
324               ELSE
325                     CODE2=10
326             END IF

327             IF (Z3T .LE. 0) THEN
328                 CODE3=3
329                 UNSTAB=1.0
330               ELSE IF (ABS(X3T) .GE. (Z3T*MU)) THEN
331                     CODE3=2
332               ELSE
333                     CODE3=1
334             END IF

335  CCCCCCCCCCCCCCCCCCCCCCCCCCCCCCCC
336  C                               C
337  C    CALCULATE CONTACT CODE     C
338  C                               C
339  CCCCCCCCCCCCCCCCCCCCCCCCCCCCCCCC

340           CODE=CODE1+CODE2+CODE3

341  CCCCCCCCCCCCCCCCCCCCCCCCCCCCCCCCCCCCCCCCCCCCCCCCCCCCCCCC
342  C                                                      C
343  C    CALCULATE THE JOINT TORQUES REQUIRED TO           C
344  C    EXERT THE FORCES X1T,Z1T,X2T,Z2T,X3T,Z3T          C
```

```
C   ON THE OBJECT.  OUTPUT THE X & Y COORDS    C
C   IF JOINT TORQUE LIMITS ARE EXCEEDED.       C
C                                              C
CCCCCCCCCCCCCCCCCCCCCCCCCCCCCCCCCCCCCCCCCCCCCCCCCCC

        TAU1=E1*X1T+E2*Z1T+E3*X2T+E4*Z2T+E5*X3T+E6*Z3T
        TAU2=E7*X2T+E8*Z2T+E9*X3T*E10*Z3T
        TAU3=E11*X3T+E12*Z3T
        X=U
        Y=RESY-V+1
        TOGL7=0
        TOGL8=0
        TOGL9=0
        IF ((TAU1 .GT. TAU1MX) .AND. (UNSTAB .EQ. 0.0)) THEN
          WRITE(13,220)X,Y
          TOGL1=1
          TOGL7=1
          ENDIF
        IF ((TAU2 .GT. TAU2MX) .AND. (UNSTAB .EQ. 0.0)) THEN
          WRITE(14,220)X,Y
          TOGL2=1
          TOGL8=1
          ENDIF
        IF ((TAU3 .GT. TAU3MX) .AND. (UNSTAB .EQ. 0.0)) THEN
          WRITE(15,220)X,Y
          TOGL3=1
          TOGL9=1
          ENDIF
        IF ((TOGL7 .EQ. 1) .AND. (CODE .EQ. 111)) TOGL4=1
        IF ((TOGL8 .EQ. 1) .AND. (CODE .EQ. 111)) TOGL5=1
        IF ((TOGL9 .EQ. 1) .AND. (CODE .EQ. 111)) TOGL6=1

CCCCCCCCCCCCCCCCCCCCCCCCCCCCCCCCCCCCCCCCCCCCCCCCCCC
C                                           C
C   OUTPUT COORDINATES TO 'SAS##.DAT' IF    C
C   THE CONTACT CODE IS 111 AND NONE OF     C
C       TORQUE LIMITS ARE EXCEEDED          C
C                                           C
CCCCCCCCCCCCCCCCCCCCCCCCCCCCCCCCCCCCCCCCCCCCCCCCCCC

        IF (((CODE .EQ. 111) .AND. (TOGL7 .NE. 1)) .AND.
     1      ((TOGL8 .NE. 1) .AND. (TOGL9 .NE. 1)))  THEN
            TOGL11=1
            WRITE(19,220)X,Y
        ENDIF

CCCCCCCCCCCCCCCCCCCCCCCCCCCCCCCCCCCCCCCCCCCCCCCCCCC
C                                              C
C   OUTPUT COORDINATES TO 'STABLE##.DAT' IF    C
C          THE CONTACT CODE = 111              C
C                                              C
CCCCCCCCCCCCCCCCCCCCCCCCCCCCCCCCCCCCCCCCCCCCCCCCCCC

        IF (CODE .EQ. 111) THEN
          WRITE(16,220)X,Y
          ENDIF
```

```
396  CCCCCCCCCCCCCCCCCCCCCCCCCCCCCCCCCCCCCCCCCCCCCCCCCCCCCCCCCCC
397  C                                                           C
398  C   DO A LEFT-TO-RIGHT SEARCH FOR CODE BOUNDARIES          C
399  C                                                           C
400  CCCCCCCCCCCCCCCCCCCCCCCCCCCCCCCCCCCCCCCCCCCCCCCCCCCCCCCCCCC

401          IF (U .EQ. 1.0) GO TO 130
402          IF ((CODE-CODEPR) .NE. 0) THEN
403            XADJ=U-0.5
404            WRITE(17,220)XADJ,Y
405            ENDIF

406  CCCCCCCCCCCCCCCCCCCCCCCCCCCCCCCCCCCCCCCCCCCCCCCCCCCCCCCCCCC
407  C                                                           C
408  C             ******STOP HERE******                         C
409  C   UPDATE CODEPR AND RETURN TO BEGINNING OF LOOP          C
410  C                                                           C
411  CCCCCCCCCCCCCCCCCCCCCCCCCCCCCCCCCCCCCCCCCCCCCCCCCCCCCCCCCCC

412  130     CODEPR=CODE
413  140     CONTINUE
414  150   CONTINUE

415  CCCCCCCCCCCCCCCCCCCCCCCCCCCCCCCCCCCCCCCCCCCCCCCCCCCCCCCCCCC
416  C                                                           C
417  C   NOW LOOK FOR HORIZONTAL BOUNDARY LINES THAT WOULD NOT   C
418  C   SHOW UP WITH A LEFT TO RIGHT TYPE OF SEARCH.  WRITE     C
419  C         THESE BOUNDARY POINTS TO 'BNDRY##.DAT'            C
420  C                ******START HERE******                     C
421  C                                                           C
422  CCCCCCCCCCCCCCCCCCCCCCCCCCCCCCCCCCCCCCCCCCCCCCCCCCCCCCCCCCC

423        IF ((ANS .NE. YES) .AND. (ANS .NE. SYES)) GO TO 180
424        CODEPR=0
425        TYPE *, 'BEGINNING TOP-TO-BOTTOM BOUNDARY SEARCH'
426        TYPE *, ' '
427        DO 180 U=1.0,RESX,1.0
428          J=RESX-U+1
429          WRITE(6,200)J
430          DO 170 V=1.0,RESY,1.0
431            XG=((U-1.0-RESX/2.0+0.5)*S*R)/(RESX/2.0-0.5)
432            YG=((1.0-V+RESY/2.0-0.5)*S*R)/(RESY/2.0-0.5)

433            P7=XG*SIN(PHI2)-YG*COS(PHI2)+R
434            P8=XG*COS(PHI2)+YG*SIN(PHI2)
435            P9=XG*SIN(PHI3)-YG*COS(PHI3)+R
436            P10=XG*COS(PHI3)+YG*SIN(PHI3)

437            Q1=P3-P1
438            Q2=P5-P1
439            Q3=P4*P2+P1*P3-P2**2.0-P1**2.0
440            Q4=P4*P1-P3*P2
441            Q5=P6*P2+P1*P5-P2**2.0-P1**2.0
442            Q6=P1*P6-P5*P2
```

```
443             R1=P4*Q3-Q1*Q4
444             R2=Q2*Q3-Q1*Q5
445             R3=P6*Q3-Q1*Q6
446             R4=P8*Q3-P7*Q4
447             R5=-1.0*Q5*P7
448             R6=-1.0*Q6*P7

449             U1=Q3*R4-Q5*R4+Q4*R5
450             U2=Q4*R6-Q6*R4
451             U3=R2*R4-R1*R5
452             U4=R3*R4-R1*R6
453             U5=Q5*R4-Q4*R5
454             U6=Q6*R4-Q4*R6

455             V1=U1*P10-U2*P9
456             V2=U3*P10-U4*P9
457             V3=U5*P10-U6*P9
458             V4=R5*P10-R6*P9

459             W1=V1/(P9*Q3*R4)
460             W2=V2/(P2*P9*Q3*R4)
461             W3=V3/(P^ Q3*R4)
462             W4=V4/(P9*R4)
463             W5=-1.0*P10/P9


464             Z3I=MG/(SQRT(W1**2+W2**2)+SQRT(W3**2+W4**2)+SQRT(W5**2+1.0))
465             X1I=W1*Z3I
466             Z1I=W2*Z3I
467             X2I=W3*Z3I
468             Z2I=W4*Z3I
469             X3I=W5*Z3I

470   CCCCCCCCCCCCCCCCCCCCCCCCCCCCCCCCCCCCCCCCCCCCCCCC
471   C                                               C
472   C   CALCULATE TOTAL CONTACT FORCES NEEDED   C
473   C          AT EACH CONTACT POINT            C
474   C                                               C
475   CCCCCCCCCCCCCCCCCCCCCCCCCCCCCCCCCCCCCCCCCCCCCCCC

476             X1T=X1E+X1I
477             X2T=X2E+X2I
478             X3T=X3E+X3I
479             Z1T=Z1I
480             Z2T=Z2I
481             Z3T=Z3I

482   CCCCCCCCCCCCCCCCCCCCCCCCCCCCCCCCCCCCCCCCCCCCCCCC
483   C                                               C
484   C   TEST FOR CONSTRAINT COMPLIANCE   C
485   C                                               C
486   CCCCCCCCCCCCCCCCCCCCCCCCCCCCCCCCCCCCCCCCCCCCCCCC

487             IF (Z1T .LE. 0) THEN
488                 CODE1=300
489               ELSE IF (ABS(X1T) .GE. (Z1T*MU)) THEN
```

```
490                     CODE1=200
491               ELSE
492                     CODE1=100
493             END IF

494             IF (Z2T .LE. 0) THEN
495                 CODE2=30
496               ELSE IF (ABS(X2T) .GE. (Z2T*MU)) THEN
497                     CODE2=20
498               ELSE
499                     CODE2=10
500             END IF

501             IF (Z3T .LE. 0) THEN
502                 CODE3=3
503               ELSE IF (ABS(X3T) .GE. (Z3T*MU)) THEN
504                     CODE3=2
505               ELSE
506                     CODE3=1
507             END IF

508   CCCCCCCCCCCCCCCCCCCCCCCCCCCCCC
509   C                             C
510   C   CALCULATE CONTACT CODE    C
511   C                             C
512   CCCCCCCCCCCCCCCCCCCCCCCCCCCCCC

513           CODE=CODE1+CODE2+CODE3

514   CCCCCCCCCCCCCCCCCCCCCCCCCCCCCCCCCCCCCC
515   C                                     C
516   C   DO A SEARCH FOR CODE BOUNDARIES    C
517   C                                     C
518   CCCCCCCCCCCCCCCCCCCCCCCCCCCCCCCCCCCCCC

519           IF (V .EQ. 1.0) GO TO 165
520           IF ((CODE-CODEPR) .NE. 0) THEN
521             YADJ=RESY-V+1.5
522             X=U
523             WRITE(17,220)X,YADJ
524             ENDIF

525   CCCCCCCCCCCCCCCCCCCCCCCCCCCCCCCCCCCCCCCCCCCCCCCCCCCCCCCCCCCCCC
526   C                                                             C
527   C              ******STOP HERE******                          C
528   C   UPDATE CODEPR AND RETURN TO BEGINNING OF LOOP            C
529   C                                                             C
530   CCCCCCCCCCCCCCCCCCCCCCCCCCCCCCCCCCCCCCCCCCCCCCCCCCCCCCCCCCCCCC

531   165     CODEPR=CODE

532   170     CONTINUE
533   180   CONTINUE
534   200   FORMAT('+',I3,' ITERATIONS REMAINING')

535   CCCCCCCCCCCCCCCCCCCCCCCCCCCCCCCCCCCCCCCCCCCCCCCCCCCCCCCCCCCCCC
```

```
C                                                       C
C   GENERATE THE CONTACT POINT DATA POINTS AND          C
C     OUTPUT THEM TO THE FILE 'CNTCTS##.DAT'            C
C                                                       C
CCCCCCCCCCCCCCCCCCCCCCCCCCCCCCCCCCCCCCCCCCCCCCCCCCCCCCCC

      X1 = RESX/2.0 + 0.5 - (RESX/(2.0*S))*SIN(PHI1)
      Y1 = RESY/2.0 + 0.5 + (RESY/(2.0*S))*COS(PHI1)
      X2 = RESX/2.0 + 0.5 - (RESX/(2.0*S))*SIN(PHI2)
      Y2 = RESY/2.0 + 0.5 + (RESY/(2.0*S))*COS(PHI2)
      X3 = RESX/2.0 + 0.5 - (RESX/(2.0*S))*SIN(PHI3)
      Y3 = RESY/2.0 + 0.5 + (RESY/(2.0*S))*COS(PHI3)

      WRITE(18,220)X1,Y1
      WRITE(18,220)X2,Y2
      WRITE(18,220)X3,Y3

CCCCCCCCCCCCCCCCCCCCCCCCCCCCCCCCCCCCCCCCCCCCCCCCCCCCCCCC
C                                                       C
C     CHECK TOGGLE SWITCHES AND OUTPUT                  C
C   WARNINGS IF JOINT TORQUE LIMITS EXCEEDED            C
C           OR SAFE AREAS EXIST                         C
C                                                       C
CCCCCCCCCCCCCCCCCCCCCCCCCCCCCCCCCCCCCCCCCCCCCCCCCCCCCCCC

      IF (TOGL1 .EQ. 1) TYPE *, 'JOINT ONE TORQUE LIMITS EXCEEDED'
      IF (TOGL4 .EQ. 1) TYPE *, 'IN STABLE AREA'
                        TYPE *, ' '
      IF (TOGL2 .EQ. 1) TYPE *, 'TOINT TWO TORQUE LIMITS EXCEEDED'
      IF (TOGL5 .EQ. 1) TYPE *, 'IN STABLE AREA'
                        TYPE *, ' '
      IF (TOGL3 .EQ. 1) TYPE *, 'JOINT THREE TORQUE LIMITS EXCEEDED'
      IF (TOGL6 .EQ. 1) TYPE *, 'IN STABLE AREA'
                        TYPE *, ' '
      IF (TOGL11 .EQ. 1) TYPE *, 'SAFE AND STABLE AREAS EXIST'

CCCCCCCCCCCCCCCCCCCCCCCCCCCCCCCCCCCCCCCCCCCCCCCCCCCCCCCC
C                                                 C
C   FORMAT FOR ALL OUTPUT DATA FILES              C
C                                                 C
CCCCCCCCCCCCCCCCCCCCCCCCCCCCCCCCCCCCCCCCCCCCCCCCCCCCCCCC

220   FORMAT(2F6.1)

CCCCCCCCCCCCCCCCCCCCCCCCCCCCCCCCCCCCCCCCCCCCCCCCCCCCCCCC
C                                                       C
C   CLOSE THE VARIOUS FILES THAT WERE OPENED            C
C                                                       C
CCCCCCCCCCCCCCCCCCCCCCCCCCCCCCCCCCCCCCCCCCCCCCCCCCCCCCCC

      CLOSE(12,STATUS='KEEP')
      CLOSE(13,STATUS='KEEP')
      CLOSE(14,STATUS='KEEP')
      CLOSE(15,STATUS='KEEP')
      CLOSE(16,STATUS='KEEP')
      CLOSE(17,STATUS='KEEP')
```

```
584         CLOSE(18,STATUS='KEEP')
585         CLOSE(19,STATUS='KEEP')

586         STOP
587         END
```

Bibliography

1. Haruhiko Asada and Jean-Jacques E. Slotine. *Robot Analysis and Control.* John Wiley and Sons, 1986.

2. David L. Brock. Enhancing the Dexterity of a Robot Hand Using Controlled Slip. In *Proc. of IEEE Int. Conf. on Robotics and Automation*, pages 249–251, 1988.

3. Mark R. Cutkosky and Paul K. Wright. Modeling Manufacturing Grips and Correlations With the Design of Robotic Hands. In *Proc. of IEEE Int. Conf. of Robotics and Automation*, volume 3, pages 1533–1539, 1986.

4. W. Holzmann and J. Michael McCarthy. Computing the Friction Forces Associated with a Three-Fingered Ggasp. *IEEE Journal of Robotics and Automation*, RA-1(4):206–210, December 1985.

5. Jeffrey Kerr and Bernard Roth. Analysis of Multifingered Hands. *The International Journal of Robotics Research*, 4(4), 1986.

6. Jeffrey Kerr and Bernard Roth. Special Grasping Configurations with Dextrous Hands. In *Proc. of IEEE Int. Conf. on Robotics and Automation*, volume 3, pages 1361–1367, 1986.

7. Richard Klafter, Thomas Chmielewski, and Michael Negin. *Robotic Engineering: An Integrated Approach.* Prentice Hall, 1989.

8. Vijay R. Kumar and Kenneth J. Waldron. Force Distribution in Closed Kinematic Chains. *IEEE Journal of Robotics and Automation*, 4(6):657–664, 1988.

9. Sundar Narasimhan. Dextrous Robotic Hands: Kinematics and Control. Master's thesis, Massachusetts Inst. of Tech., November 1988. Dept. of Elect. Eng. and Comp. Sci.

10. Van-Duc Nguyen. Constructing Force Closure Grasps. In *Proc. of IEEE Int. Conf. on Robotics and Automation*, volume 2, pages 1368–1373, 1986.

11. No author given. Hand Electronics Documentation Package. Technical report, Sarcos Incorporated, 274 South 1200 E. Salt Lake City, Utah 84102, March 1987.

12. J.K. Salisbury and B. Roth. Kinematic and Force Analysis of Articulated Mechanical Hands. *Journal of Mechanisms, Transmissions, and Automation in Design*, 105:35–41, 1983.

Vita

Stephen G. Edwards [redacted] In July, 1978 he moved with his family to Kailua, Hawaii on the island of Oahu. He graduated with honors from Iolani School in 1982, and went on to attend the United States Air Force Academy. As a cadet he received several awards for academic achievement, and successfully completed the Academy's honors program. He graduated in 1986 with a Bachelor of Science in Astronautical Engineering, specializing in navigation, guidance, and control systems.

As a lieutenant his first assignment was to the 6595th Test & Evaluation Group at Vandenberg AFB, Ca. While at Vandenberg he worked on several flight test programs including the air-launched anti-satellite missile (ASAT), the Space-Based Interceptor, and the Peacekeeper ICBM. After three years at Vandenberg he entered the Air Force Institute of Technology in May, 1989.

[redacted]

REPORT DOCUMENTATION PAGE

Form Approved
OMB No. 0704-0188

1. AGENCY USE ONLY (Leave blank)	2. REPORT DATE	3. REPORT TYPE AND DATES COVERED
	27 Nov 90	Master's Thesis

4. TITLE AND SUBTITLE
Use of Grasp Force Focus Positioning to Enhance the Torque Resistance Capability of Robotic Grasps

5. FUNDING NUMBERS

6. AUTHOR(S)
Stephen G. Edwards, Capt, USAF

7. PERFORMING ORGANIZATION NAME(S) AND ADDRESS(ES)
Air Force Institute of Technology
Wright-Patterson AFB, OH 45433-6583

8. PERFORMING ORGANIZATION REPORT NUMBER

9. SPONSORING/MONITORING AGENCY NAME(S) AND ADDRESS(ES)

10. SPONSORING/MONITORING AGENCY REPORT NUMBER

11. SUPPLEMENTARY NOTES

12a. DISTRIBUTION/AVAILABILITY STATEMENT
Approved for public release, distribution unlimited

12b. DISTRIBUTION CODE

13. ABSTRACT (Maximum 200 words)

Three-point-contact grasps are unique in that the homogeneous solution for the contact forces always produces a grasp force focus. Careful positioning of this focus point in the grasp plane can help avoid two things; slipping at the contact points, and violation of joint torque limits. The focus placement method is explored theoretically by examining two types of grasps on cylinders; 1) fingertip grasps using three independently operated fingers, and 2) single-finger power grasps with one contact point on each of three links. Constraint maps are generated for various fingertip grasps in order to show how proper placement of the grasp force focus results in no-slip grasps. A specific single-finger power grasp, using a specific manipulator, is examined in order to show that joint torque limits also affect focus placement. The results show that optimal focus location is grasp-specific, and that torque direction also plays a role in the torque resistance capability of the grasp.

14. SUBJECT TERMS	15. NUMBER OF PAGES
Robotics, Grasping, Internal contact forces, Grasp force focus	101
	16. PRICE CODE

17. SECURITY CLASSIFICATION OF REPORT	18. SECURITY CLASSIFICATION OF THIS PAGE	19. SECURITY CLASSIFICATION OF ABSTRACT	20. LIMITATION OF ABSTRACT
Unclassified	Unclassified	Unclassified	UL